GREW CREEK EPITHERMAL GOLD-SILVER DEPOSIT, TINTINA TRENCH, YUKON, (105K/2)

Anthony B. Christie,
DSIR Geology and Geophysics
P.O. Box 30-368,
Lower Hutt, New Zealand

Jesse L. Duke,
Noranda Exploration Company Limited,
Suite 203-107 Main Street,
Whitehorse, Yukon,
Y1A 2A7

and

Ralph Rushton,
Department of Geology,
University of Alberta,
Edmonton, Alberta
T6G 2E3

CHRISTIE, A.R., 1992. Grew Creek epithermal gold-silver deposit, Tintina Trench, Yukon. In: Yukon Geology, Vol. 3; Exploration and Geological Services Division, Yukon, Indian and Northern Affairs, Canada, p.223-259

ABSTRACT

The Grew Creek epithermal gold-silver deposit in southeast Yukon (MINFILE 105K 009) is hosted by Eocene volcanic and sedimentary rocks deposited in a pull-apart basin within the Tintina Fault Zone. Flow rhyolites forming a dome in the Tarn Zone area, 1.5 km east of Grew Creek, pass westward into a succession of rhyolitic ignimbrites and air fall tuffs, exposed along Grew Creek and in the Main Zone, 500 m west of Grew Creek. These rhyolitic rocks are faulted against fluvial sediments to the north, along the W-E Fault, and basaltic rocks to the west. In the Main Zone, the volcanics, sediments, and the W-E Fault all dip steeply to the north.

The gold-silver mineralization forms an elongate tabular zone within the rhyolitic tuffs. The zone strikes parallel to the W-E Fault and dips vertically or steeply to the north. The eastern end of the mineralized zone is defined by a decrease in grade, whereas the western end is faulted off against the basaltic rocks. Within the zone, stockwork veins and hydrothermal breccias contain assemblages which include quartz, adularia, carbonates, quartz pseudomorphous after calcite, pyrite, marcasite, and traces of arsenopyrite, chalcopyrite, acanthite, electrum, silver selenides, galena, and sphalerite.

There is good correlation between gold and silver in drill core assays, with a gold:silver ratio of around 1:4 for the ore grade mineralization. The mineralization is strongly anomalous in arsenic and mercury, but there is only a weak correlation of mercury with gold and silver, with most high values for mercury lying above the gold-silver zone and associated with the W-E Fault. Arsenic concentrations are elevated over much of the area but there is no statistical correlation with the locally high concentrations of gold or silver.

Outcropping rhyolitic rocks are hydrothermally altered to intermediate argillic and advanced argillic assemblages, whereas subsurface rhyolitic rocks are altered to quartz-adularia or illite-quartz assemblages adjacent to veins, and to illite-quartz-adularia ± carbonate elsewhere. Advanced illite-quartz-adularia ± carbonate alteration is accompanied by an increase in Na_2O and decreases in TiO_2, CaO and Al_2O_3. Basalts are altered to carbonate-chlorite (propylitic) assemblages, accompanied at an advanced stage by a slight increase in CaO, and decreases in K_2O, Na_2O, SiO_2, and Al_2O_3.

Mineralization postdated tilting of the host pyroclastic and sedimentary rocks. Episodic fault movements in the Tintina Fault Zone structurally focused the hydrothermal fluids by providing locally high secondary permeability, whereas the high primary permeability of the rhyolitic tuffs promoted the development of stockwork veins and breccias. The absence of significant alteration and mineralization in the sediments suggests that a partly welded and intensely altered tuff unit, along the footwall of the W-E Fault, acted as an aquiclude, confining the hydrothermal fluid within the rhyolitic tuffs. Intense pyritic alteration of this unit and high concentrations of mercury in the vicinity of the W-E Fault form pyrite and mercury zones north of the mineralization.

RÉSUMÉ

Le gisement épithermal d'or et d'argent Grew Creek, au sud-est du Yukon, se trouve dans des roches volcaniques et sédimentaires de l'Éocène déposées dans un bassin d'extension situé à l'intérieur de la zone faillée de Tintina. Des coulées de rhyolites provenant d'un dôme dans la région de la zone Tarn, à 1,5 km à l'est du ruisseau Grew passent vers l'ouest à une succession d'ignimbrites et de projections de tufs rhyolitiques qui sont mis à nu le long du ruisseau Grew et dans la zone Main, à 500 m à l'ouest du ruisseau Grew. Ces roches rhyolitiques sont faillées et reposent contre des sédiments fluviaux au nord, le long de la faille W-E, et contre des roches basaltiques à l'ouest. Dans la zone Main, les roches volcaniques et sédimentaires et la faille W-E présentent un fort pendage en direction du nord.

La minéralisation en or et en argent forme une zone tabulaire à l'intérieur des tufs rhyolitiques. La zone est orientée parallèlement à la faille W-E et présente un pendage vertical ou abrupt en direction du nord. L'extrémité orientale de la zone minéralisée est définie par une diminution des teneurs alors qu'à son extrimité occidentale elle est séparée des roches basaltiques par une faille. À l'intérieur de la zone, un réseau de veines minéralisées et des brèches hydrothermales renferment des assemblages englobant du quartz, de l'adulaire, des carbonates, du quartz pseudomorphe de la calcite, de la pyrite, de la marcasite et des traces d'arsénopyrite, de chalcopyrite, d'acanthite, d'electrum, de séléniures d'argent, de galène et de sphalérite.

Il existe une bonne corrélation entre les déterminations des teneurs en or et en argent dans des carottes de forages et le rapport or sur argent est d'environ 1:4 pour la minéralisation à teneur commerciale. La minéralisation présente des concentrations fortement anormales en arsenic et en mercure, mais le mercure ne présente qu'une faible corrélation avec l'or et l'argent. La plupart des concentrations élevées en mercure ont été relevées au-dessus de la zone aurifère et argentifère et sont associées à la faille W-E. Les concentrations en arsenic sont élevées sur une bonne partie de la région, mais ne présentent aucune corrélation statistique avec les concentrations élevées par endroits en or et en argent.

Les roches rhyolitiques affleurantes ont été hydrothermalement altérées en assemblages argilliques intermédiaires à avancés, alors que les roches rhyolitiques subsuperfricielles sont altérées en assemblages de quartz-adulaire ou de quartz-illite près des veines et en illite-quartz-adulaire ± carbonate ailleurs. Une altération poussée en illite-quartz-adulaire ± carbonate s'accompagne d'accroissements des concentrations en Na_2O et de diminutions des concentrations en TiO_2, en CaO et en Al_2O_3. Les basaltes sont altérés en assemblages de carbonate et chlorite (propylitiques) avec un léger accroissement de la concentration en CaO et des diminutions des concentrations en K_2O, en Na_2O, en SiO_2 et en Al_2O_3.

La minéralisation est postérieure à l'inclinaison des roches pyroclastiques et sédimentaires hôtes. Des déplacements épisodiques le long des failles dans la zone faillée de Tintina ont concentré les fluides hydrothermaux en fournissant des perméabilités secondaires élevées par endroits alors que la perméabilité primaire élevée des tufs rhyolitiques favorisait la formation du réseau de veines et des brèches. L'absence d'une altération importante et d'une minéralisation dans les sédiments suggère qu'une unité partiellement soudée de tuf ayant subi une intense altération, le long de la lèvre inférieure de la faille W-E, a agi comme une aquiclude confinant les fluides hydrothermaux aux tufs rhyolitiques. Une intense altération pyriteuse de l'unité de tuf rhyolitique et des concentrations élevées en mercure sont observées aux environs de la faille E-W au nord de la minéralisation.

INTRODUCTION

The Grew Creek prospect (MINFILE 105K 009) is a volcanic-associated epithermal gold-silver deposit located about one kilometre south of the Robert Campbell Highway, half way between Faro and Ross River, in south-east Yukon (Fig. 1A; NTS 105 K/2 115815; Latitude 62°03'N and Longitude 132°50'W). The prospect has been of considerable interest to the exploration industry because it was the first reported showing of epithermal mineralization in the Tintina Trench. Lesser showings have since been discovered near Dawson (Mortensen, 1988) and Glenlyon (Pride, 1988). We commenced this study in 1988 with the aims of characterizing the geology of the deposit and determining its genesis, building on previous descriptions of the deposit by Duke (1986), and Duke and Godwin (1986), but using a much larger database of drillhole information. This paper reports preliminary results of our work. Oxygen isotope analyses of vein and wall rock samples, and petrographic work, are continuing.

EXPLORATION HISTORY

Mineralization was discovered in outcrop, 600 m west of Grew Creek, by prospector Al Carlos in 1983 while exploring for a possible source of the previously known placer gold in Grew Creek. He reported an assay of 10 grams gold/tonne (g/t Au) across the discovery outcrop. Hudson Bay Exploration and Development Company Limited (Hudson Bay) optioned the property in November 1983 and carried out geological, geophysical and geochemical surveys, trenching, 1,732 m of diamond drilling in 13 holes, and 1,660 m of rotary drilling in 19 holes (Anon, 1985; Stroshein, 1986a, 1986b). An area of gold-silver mineralization, named the Main Zone, was defined around the discovery outcrop (10062E/9945N on the Noranda grid, see below) and centred approximately 500 m west of Grew Creek. An area of extensive hydrothermal alteration and anomalous geochemistry centred approximately 1.5 km east of Grew Creek, was named the Tarn Zone (Figs 1C and 2). Hudson Bay dropped its option in January 1987, and a new option agreement was taken up by Noranda Exploration Company Limited (Noranda) in June 1987. Golden Nevada Resources Incorporated (Goldnev) and Brenda Mines farmed into the property in June 1987, by funding the subsequent exploration program operated by Noranda. During 1987 and 1988 Noranda carried out geological mapping, as well as ground based magnetometer, induced polarization (IP)/resistivity and soil geochemistry surveys, an airborne electromagnetic survey, 235 m of trenching, 19,173 m of diamond drilling in 77 holes, and 1,651 m of reverse circulation drilling in 13 holes (Copland, 1988a, 1988b; Duke, 1988). Noranda defined the Main Zone mineralization as an east-west orientated body up to 550 m long, 110 m wide and 150 m deep. No significant mineralization was encountered in the Tarn Zone but additional drill targets near the Main Zone were identified. Subsequently, Goldnev became operator and, during 1989, drilled 10 diamond drillholes totalling 1,164.5 m in the Main Zone, to further define the ore reserves (Seto and Crowe, 1989).

The airborne geophysical surveys proved useful as an aid to interpreting regional structure and geology, and the IP/resistivity anomalies defined depth of overburden. However, the thick cover of till appears to have masked the detailed trends of the mineralization. On a regional scale, the mineralization is characterized by anomalous arsenic and mercury soil (till) geochemistry, but these anomalies are broad and failed to define drill targets in the mineralized zone.

ORE RESERVES

Orcan Mineral Associates estimated geological reserves of 852,100 short tons (773,012 tonnes) grading 0.260 oz/ton Au (8.9 g/t Au) and 0.98 oz/ton Ag (33.6 g/t Ag) at a cut-off grade of 0.058 oz/ton (0.2 g/t), and containing a higher grade reserve of 203,870 short tons (184,947 tonnes) grading 0.354 oz/ton Au (12.1 g/t Au) (Goldnev news release, December 4, 1989).

PREVIOUS RESEARCH WORK

Duke (1986) and Duke and Godwin (1986) mapped and sampled Grew Creek, the discovery outcrop, and several of Hudson Bay's exploration trenches, and carried out mineralogical, geochemical, oxygen isotopic, and K-Ar age analyses and petrographic work. They demonstrated that the mineralization consisted of gold, electrum, pyrite, and silver selenide minerals in quartz and K-feldspar veins hosted by rhyolitic tuffs. Silicic, acid sulphate, and argillic acid sulphate hydrothermal alteration types were identified in trenches and surface outcrops, and found to be overprinted by "surficial alteration" weathering. K-Ar ages on least altered basalts (51.4 and 50.7 m.a. B.P.) and palynological ages on mudstones (age range representing 56 to 46 m.a. B.P.) associated with the rhyolitic tuffs indicated a mid Eocene age for the host rocks, whereas three K-Ar ages on hydrothermally altered tuffs (51.5, 47.0 and 36.0 m.a. B.P.) suggested a mid to late Eocene age for the mineralization. A deep magmatic source for the mineralization was postulated based on the degree of heavy oxygen isotope enrichment.

Jackson et al. (1986) and Pride (1988) described the basalt and rhyolite associated with the Tintina Fault, including those at Grew Creek, and reported XRF analyses and several whole rock K-Ar ages. Jackson et al. (1986) concluded that the volcanic rock suite was strongly bimodal, with calc-alkaline to transitional tholeiitic basalts and high potassic subaluminous rhyolites. The basalts were dated as Eocene (5 K-Ar ages ranging from 55.4 to 46.4 m.a. B.P.) and the rhyolites as Paleocene to Eocene (4 K-Ar ages ranging from 58.2 to 51.5 Ma).

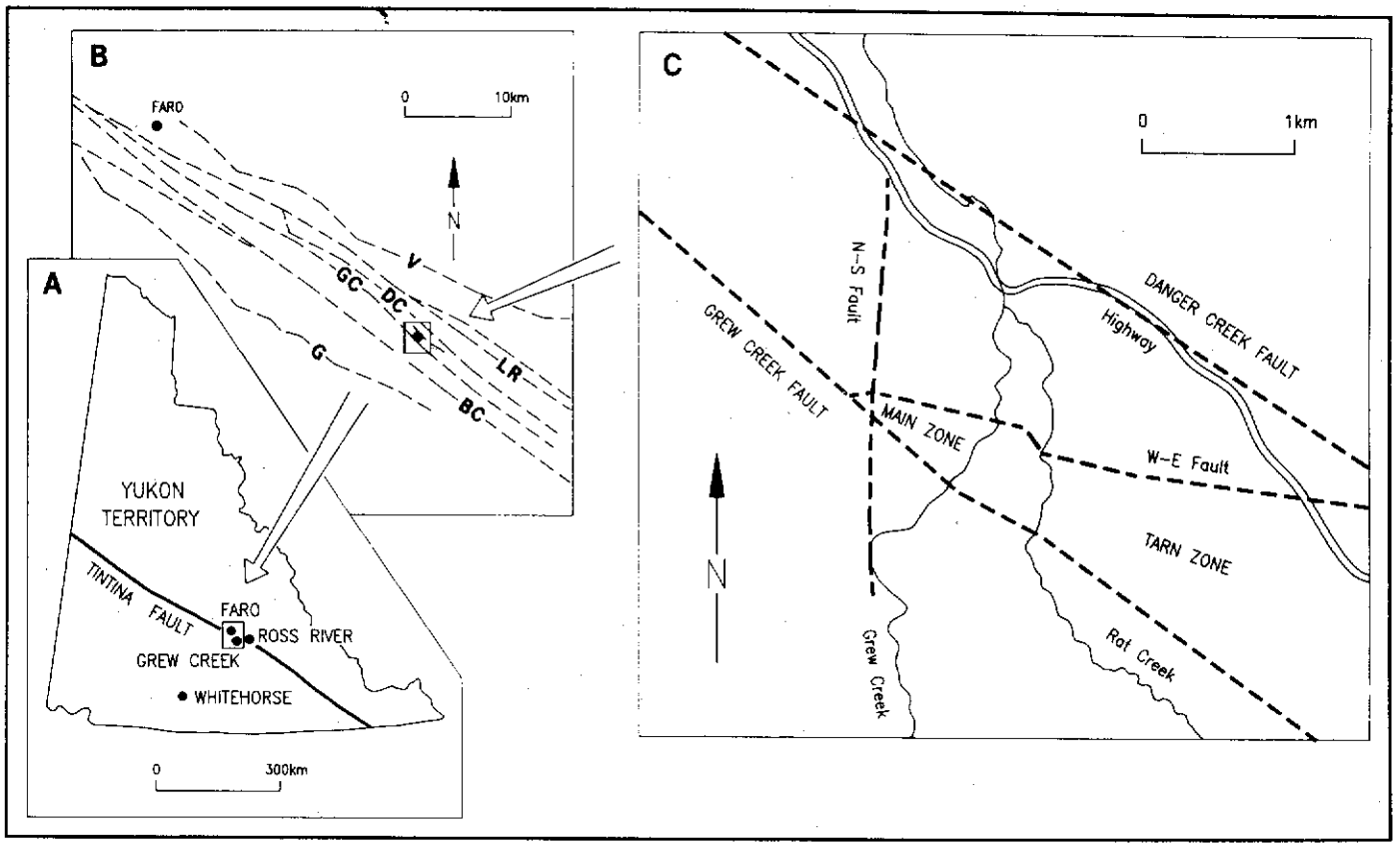

Figure 1. Maps showing the location of the Grew Creek gold-silver deposit on the Tintina Fault Zone in south-eastern Yukon Territory (Figure 1A), the component faults of the Tintina Fault Zone in the Grew Creek area (Figure 1B), and the location of the deposit within the fault zone (Figure 1C). In Figure 1B, BC = Buttle Creek Fault, DC = Danger Creek Fault, G = Glenlyon Fault, GC = Grew Creek Fault, LR = Lapie River Fault and V = Vangorda Fault.

METHODOLOGY

Field work for this study was carried out during the 1988 summer. Duke was the Noranda Project Geologist at Grew Creek, whereas Christie made a one week visit in May to define the project and a six week visit with Rushton, during July and August, to relog drill core, and map and collect surface samples from outcrop. Thirty nine of the total of 90 diamond drillholes (in 1988) were relogged using a scheme that emphasized descriptive features that were considered helpful in correlating the pyroclastic units (e.g. quantity, grain size and texture of the crystal, lithic, pumice and matrix components). These logs were used, in conjunction with Noranda drill logs, to construct 1:500 scale vertical cross-sections (listed by coordinates in Fig. 3) and a longitudinal stratigraphic section through the Main Zone. Samples representative of the different lithological units were collected and 70 were later examined in thin section. Forty-eight samples were analysed for mineralogy, and major and trace elements, using XRD, XRF and ICP techniques respectively (Appendix).

Drillhole descriptive logs, downhole assay data, drill sections, maps and geophysical results were made available by Noranda. The Noranda drillhole descriptive logs were used to prepare hand plotted cross-sections, individually showing veins, visually estimated percent pyrite concentration, and intensity and type of hydrothermal alteration, for eight cross-sections through the Main Zone (listed by coordinates in Fig. 3).

GEOLOGIC AND STRUCTURAL SETTING

The Grew Creek deposit occurs in the Tintina Fault Zone, a transcurrent fault more than 1000 km long which crosses Yukon Territory (Fig. 1), and extends into Alaska to join the Kaltag Fault, and into British Columbia to join the Rocky Mountain Trench Fault. Displacement, crushing and erosion of rocks along the Tintina Fault Zone have formed a major linear physiographic depression termed the Tintina Trench. Dextral displacement of rock units either side of the fault zone indicates transcurrent movement of more than 500 km, mostly during the Late Cretaceous and Tertiary. In the Grew Creek area, rocks of the Pelly-Cassiar Platform to the southwest are juxtaposed against rocks of the Anvil Allochthon to the northeast. Pull-apart basins were formed along the fault zone where it expanded into braided sections, and these were the locus of sedimentation and bimodal basaltic-rhyolitic volcanism

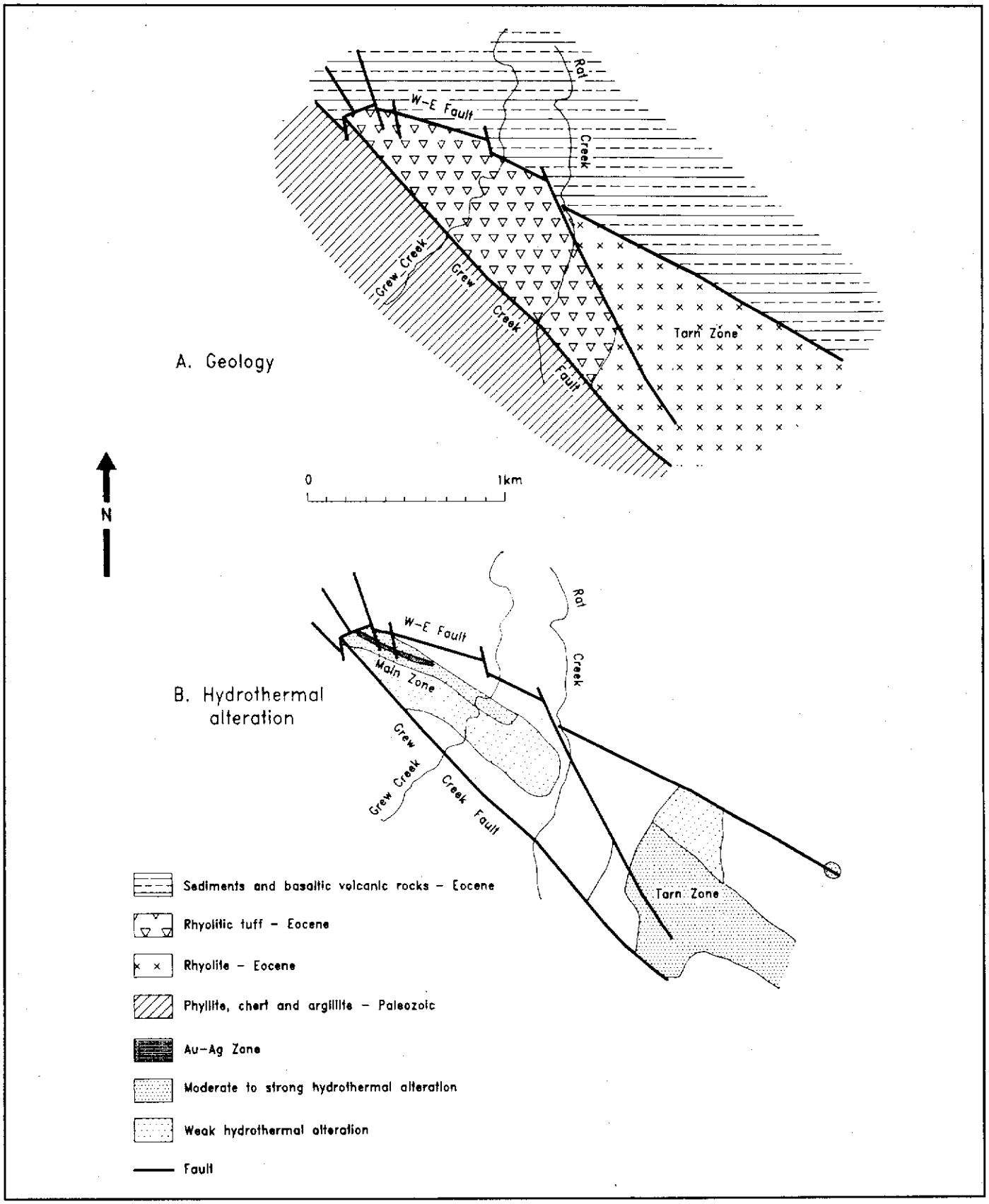

Figure 2. Grew Creek prospect geology (Figure 2A) and hydrothermal alteration (Figure 2B) maps (modified after Duke, 1988).

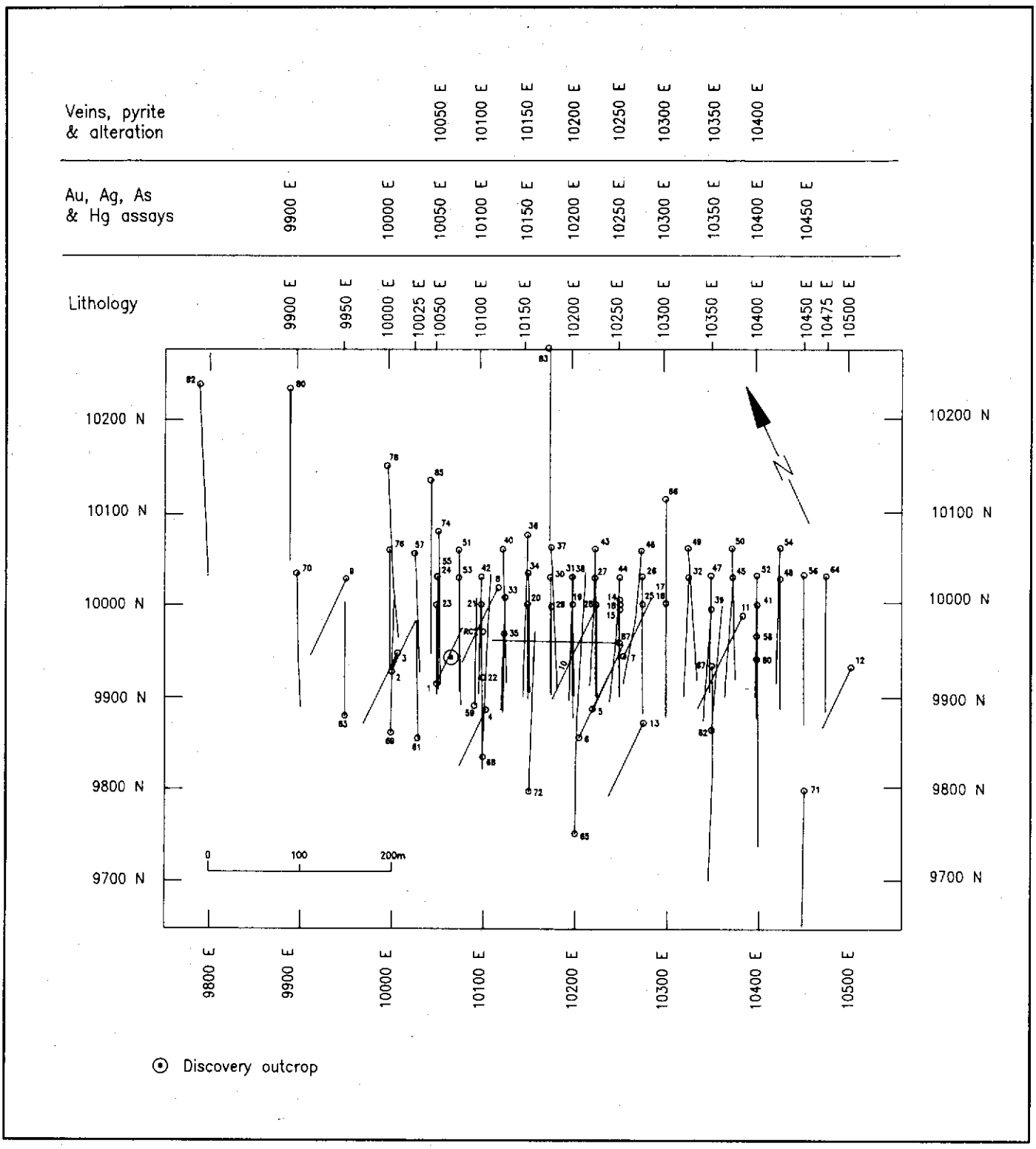

Figure 3. Map of drillhole locations on the Noranda exploration grid in the Main Zone. The grid is orientated at 019°/109°. All drillholes shown are angled diamond drillholes (generally 45° or 55° dip). The rows of section numbers above the diagram note the sections on which the following work was carried out: 1. veins, pyrite and alteration row = sections on each grid line were hand plotted from information in Noranda's descriptive drill logs, to show veins, visually estimated percent pyrite concentration, and intensity and type of hydrothermal alteration, 2. Au, Ag, As & Hg assays row = assay sections were computer plotted and examined, and 3. Lithology row = drillholes in these sections were relogged.

during the Eocene (Christie and Gordey, 1989; Pride, 1988; c.f. Hughes and Long, 1980). Subsequent differential uplift and erosion has exposed some of these Eocene rocks, preserved in graben within the Tintina Trench.

In the Grew Creek area, the Tintina Fault Zone includes at least six major faults; namely, from north to south: Vangorda, Lapie River, Danger Creek, Grew Creek, Buttle Creek, and Glenlyon (Fig. 1B). The Grew Creek prospect lies on the northern side of the Grew Creek Fault, on the south side of the Tintina Trench. Duke (1988) considered that the Main Zone is located where the Grew Creek Fault is intersected by a north-south extensional fault (N-S Fault in Fig. 1C), defined by a physiographic linear feature.

The Grew Creek area is covered with Quaternary glacial till, typically 50 m thick, which limits bedrock exposures to the creeks and rare exposures elsewhere, such as the discovery outcrop. The northwest striking Danger Creek and Grew Creek faults enclose a 1.5 km wide graben (Canyon Graben; Stroshein 1986b) of Eocene sedimentary and volcanic rocks. The faults separate the graben from Triassic metabasalt and limestone to the north, and from Paleozoic phyllite, argillite and chert to the south. A west-northwest striking fault (hereafter termed the W-E Fault) subdivides the Eocene rocks into a northern sequence of fluvial sedimentary rocks intercalated with basaltic pyroclastic and epiclastic rocks, and a southern sequence of rhyolitic volcanic rocks (Fig. 2A). To the east, the rhyolitic rocks consist predominantly of dome facies rhyolite flows and quartz feldspar porphyries, which pass westward into a succession of rhyolitic pyroclastic rocks exposed along and west of Grew Creek. Basalt and rhyolite dykes intrude both the volcanic and sedimentary sequences. From the Main Zone northwards, the tuffs, sediments, and intervening W-E Fault all dip about 80° to the north (Fig. 4A) so that a plan view transect (Fig. 2A) approximates a stratigraphic section.

PROSPECT STRUCTURE

In the Main Zone, drillhole intersections of the Grew Creek Fault define a more than 10 m wide zone of unconsolidated gouge and rock fragments. The W-E Fault is represented by shearing along the sedimentary-volcanic rock contact, sometimes with fault gouge developed. Many other faults have been intersected in the Main Zone drillholes, some with wide clay gouge zones and others represented by tectonic breccias. Duke (1988) correlated some of these intersections with air photo lineaments, and magnetic and IP/resistivity anomalies. He postulated the presence of six north to northwest-striking extensional faults, and several small northeast striking faults within the Main Zone, to account for displacements in the stratigraphy and jogs in the W-E and Grew Creek faults (Figs 2 and 5).

Severely broken core in mineralized vein and breccia zones indicates that many of the mineralized structures have been tectonically reactivated since cessation of mineralization.

DETAILED PROSPECT GEOLOGY

We constructed a stratigraphic column for each of the drillhole cross-sections by assuming that dip was a constant 80°, and by correlating and projecting the drillhole information onto a plane dipping 10° south and passing through a pivot on the 9950N grid line at an elevation of 700 m (equivalent to a depth of 90-145 m). These columns were assembled to produce a stratigraphic section for the Main Zone at 1:500 scale, simplified and reproduced here at smaller scale in Fig. 5. This section illustrates the relationships of the rhyolitic and basaltic volcanic rock, and fluvial sedimentary rock sequences, and subdivides the rhyolitic sequence into a number of composite pyroclastic units. Lateral variations in thickness and pinching of units in the rhyolitic sequence, and the jagged trace of the W-E Fault, may be caused by changes in dip along the section (not compensated for) and displacements on several north and northwest striking faults (see Structure section above). Additionally, several primary volcanic facies features may also contribute to the lateral variations, including: (a) rapid thickening and thinning caused by draping over existing topography, and valley filling, (b) erosion and production of epiclastites, and (c) overlapping volcanic centres.

Rock types

(a) Rhyolite and felsic porphyries

Coarse grained "quartz eye" porphyritic rhyolite outcrops along a prominent ridge from Rat Creek southeast to Danger Creek. Porphyritic rhyolites, including quartz-feldspar, quartz-eye, and feldspar "porphyries", are the main lithologies in the Tarn Zone drillholes and occur elsewhere in the sedimentary and volcanic sequences as dykes. Many of the dykes in the Main Zone logged by Noranda geologists as rhyolite and quartz feldspar porphyry proved to be hydrothermally altered basalt ("rhyolite"), vitric ash tuff ("rhyolite"), or partly welded lapilli tuff ("quartz feldspar porphyry") when examined in thin section. In the Main Zone there is a semi-continuum of textures from "quartz feldspar porphyry" to partly welded, crystal vitric lapilli ash tuff with pseudo quartz-feldspar porphyry macro-texture but containing some welded shards and pumice. These pseudo-porphyries may have been formed by melting and remobilization of basal pyroclastic units.

Samples of Tarn Zone rhyolite from DDH 90 contain about 40% phenocrysts, up to 4 mm in diameter, of plagioclase (euhedral), sanidine, quartz and a mafic mineral, in a groundmass recrystallized to quartz, K-feldspar and illite. Flow banding and spherulitic textures are developed locally. Quartz-feldspar porphyry is similar to rhyolite but with larger phenocrysts and well developed flow banding. Large quartz "eyes" are prominent in altered examples.

(b) Rhyolitic pyroclastites

Rhyolitic tuffs are the most important lithology in economic terms, as they host the Main Zone mineralization.

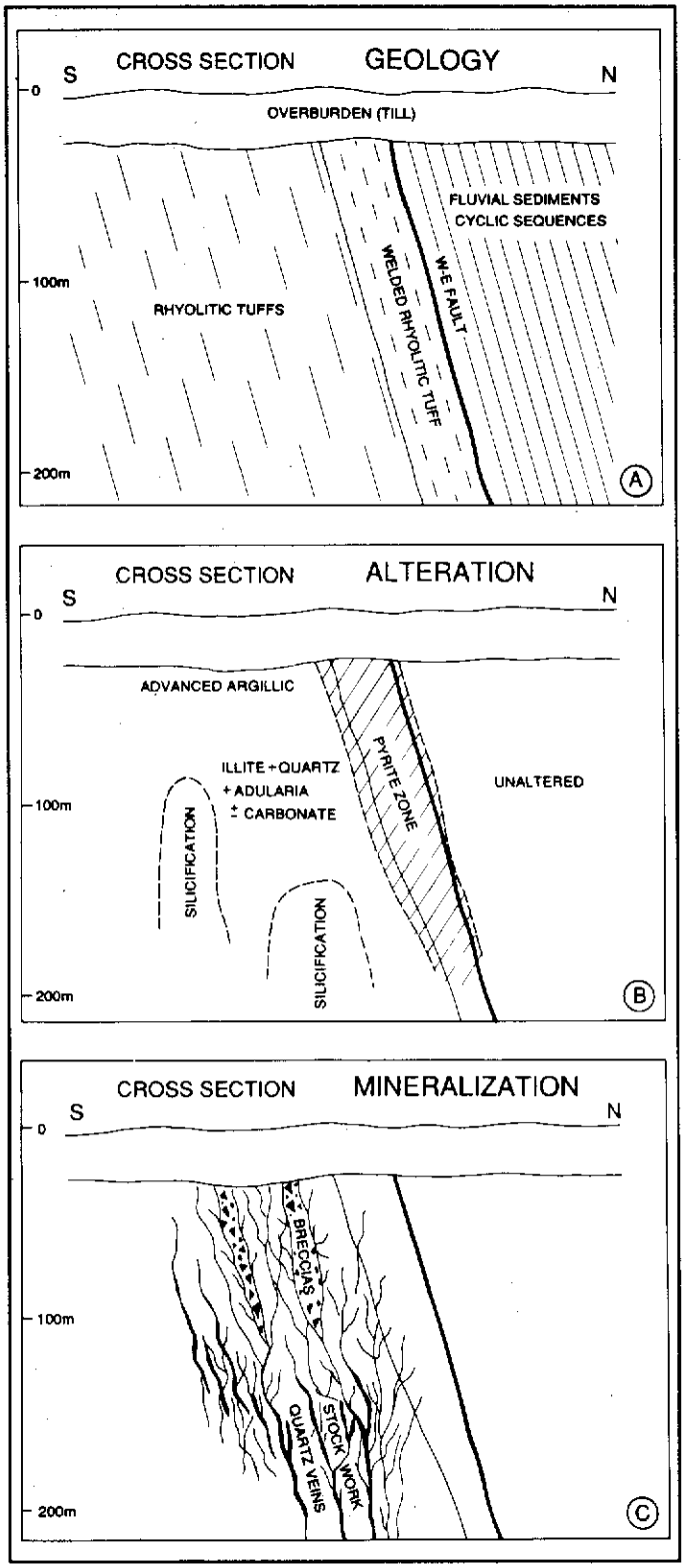

Figure 4. Diagrammatic cross-sections through the main zone illustrating geology (Figure 4A), hydrothermal alteration (Figure 4B), and mineralization (Figure 4C).

They are exposed in the creeks and were intersected by the Main Zone drillholes, south of the W-E Fault (Figs 2A, 4A and 5), and can be grouped into the following three major types, based on grain size and composition (Table 1 and Fig. 6):

1. S&P (salt & pepper) tuff: S&P tuff comprises "crystal- and lithic-rich" mixed coarse ash tuff, lapilli-ash tuff and lapilli tuff with a distinctive, well sorted granular "salt & pepper" appearance (Fig. 7). These are the crystal lithic tuffs described by Duke and Godwin (1986) from exposures along Grew Creek. They mapped six depositional units based on cyclic increases in grain size northward down the creek (up the stratigraphic sequence). We have identified more than 12 units of S&P tuff in the eastern drillholes of the Main Zone with contacts marked by major changes in grain size or tuff type (e.g. interbedded thin units of VA tuff or CLP tuff, see below). Each unit is internally homogeneous and no sedimentary structures were observed. The upper part of the S&P sequence contains only "fine" grained S&P units (crystals and lithics average about 1.5 mm), whereas several coarse grained S&P units (crystals and lithics averaging 3 mm) are present in the lower part.

2. CLP (crystal lithic pumice) tuff: CLP tuffs are "glass-rich" coarse ash tuff and lapilli-ash tuff (Figs 8 and 9) which occur mostly in the upper part of the rhyolitic sequence and dominate the western end of the section (Fig. 5). Three major types are identified: (a) non-welded coarse ash tuff, (b) non-welded lapilli-ash tuff, and (c) welded or partly welded lapilli ash tuff (logged by Noranda as quartz-feldspar porphyry). Two units of non-welded CLP tuff on section 1000E are separated by a 40 cm thick unit of trough cross bedding (Fig. 10), representing either a basal surge layer or an epiclastite.

3. VA (vitric ash) tuff: VA tuff (Figs 11 and 12) is characterized by having more than 75% glass ash matrix and pumice fragments. It generally occurs as thin units separating units of S&P tuff and/or CLP tuff.

In all three types of tuff, the crystal fragments are mainly quartz and lesser feldspar (mostly sanidine), whereas the lithics are mostly fragments of rhyolitic tuff and rhyolite flows, and lesser basalt, shale, phyllite, and diabase (dolerite). The lithics generally have a coarser average grainsize than the crystals, and in some samples there is a bimodal grain size distribution of crystals with the finer population predominating. Pumice exhibits a considerable range in grain size, averaging 3-5 mm in diameter, but commonly around 1 cm, with rare blocks up to 25 cm in diameter (Fig. 8). The glass matrix is generally too fine grained, hydrothermally altered and/or recrystallized to identify components, but good examples of glass shard textures are present in some samples (e.g. 8/34.1m, 10/81.1m, 18/159.6m, 47/100.8m, 59/99.65m, 60/271m 65/346.5m, and 85/333.4m; Fig. 12). Some CLP and VA tuffs are welded (e.g. 47/79.95m, 60/271m, 65/346.5m, RR19, and TR1) with flattening of pumice

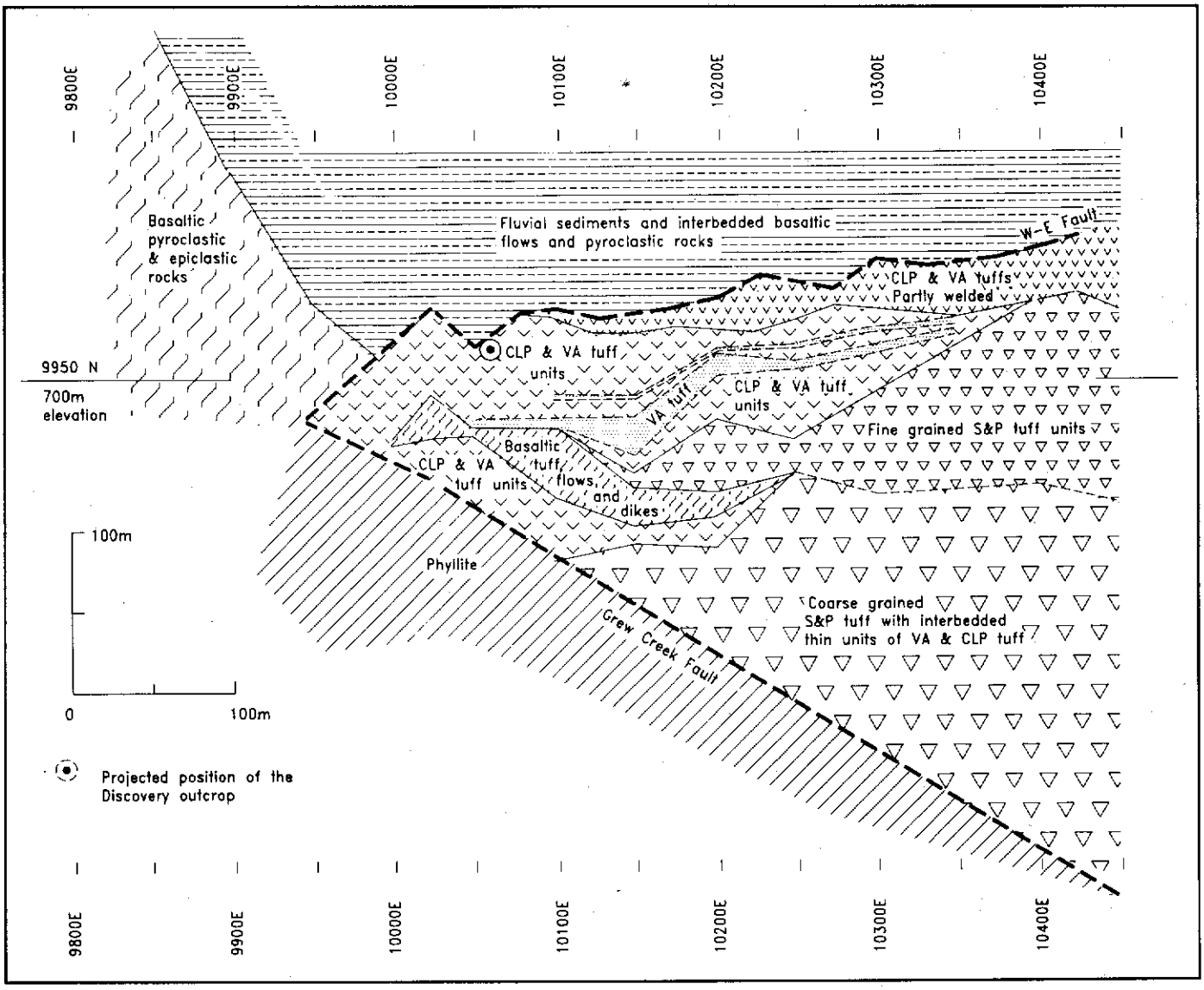

Figure 5. Stratigraphic section through the Main Zone constructed on a plane dipping 10° southward and passing through section 9950N (Figure 2) at an elevation of 700 m. See Table 1 for definitions and descriptions of CLP, S&P and VA tuffs.

fragments and glass shards, and the development of a eutaxitic texture in the glass (+shard) groundmass. Welding and hydrothermal alteration of some CLP tuff units has produced an appearance similar to quartz feldspar porphyry and led to the misidentification of these units as dykes, particularly the "quartz feldspar porphyry" noted on the footwall of the W-E Fault by Duke (1988), Christie and Gordey (1989), Christie et al. (1989), which in reality is the uppermost CLP tuff unit (Fig. 5).

(c) Fluvial sediments

Clastic sedimentary rocks ranging from conglomerates to claystones occur north of the W-E Fault. They are exposed in Grew Creek, northeast of the Tarn Zone, and in a small quarry north of the Highway, and were intersected in many of the drillholes (Figs 2, 4 and 5). The sediments generally dip steeply north but are folded in Grew Creek and the quarry area, near the Robert Campbell Highway (e.g. see Fig. 12 of Pride 1988). Bedding is marked by changes in grain size, whereas a lamination is defined by alternating pale low density mineral and dark higher density mineral bands in some of the sandstones and finer sediments. The coarser beds contain logs and twigs, and beds of coal are associated with some fine grained units.

The conglomerates are clast supported, polymictic, and moderately to poorly sorted. The clasts are typically about 4 cm in diameter, up to a maximum of 15 cm in diameter, and set in a coarse sandy matrix. Clast lithologies include schist, quartz vein material, felsic and mafic volcanic rocks, chert, and quartzite.

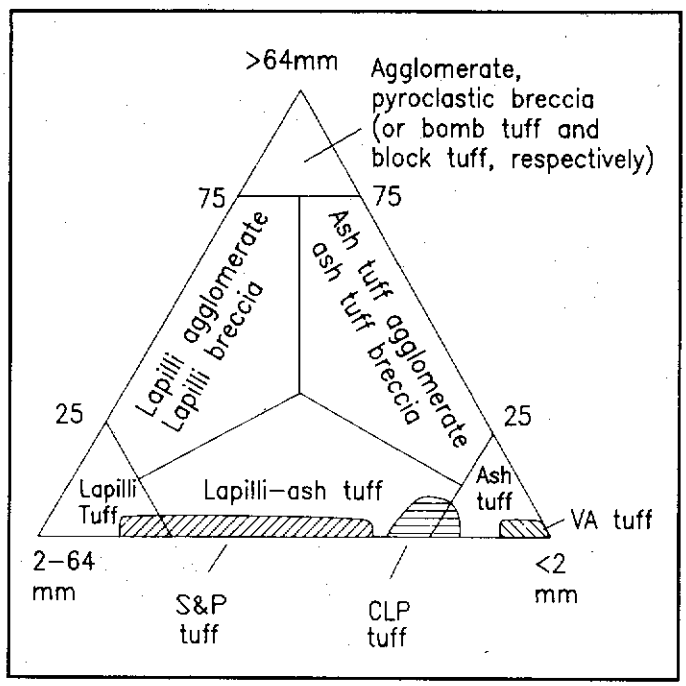

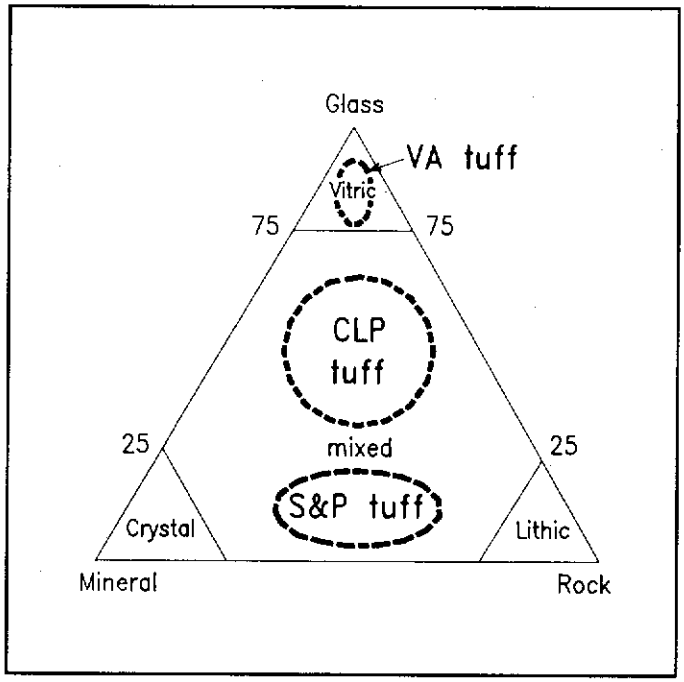

Figure 6. Relative compositions of the S&P, CLP, and VA rhyolitic tuffs (Table 1) plotted on pyroclastic rock classification ternary diagrams from Dietrich & Skinner (1979).

Drillhole sections through the sediments in the Main Zone typically exhibit fining upward cycles from conglomerate, through pebbly sandstone, sandstone, siltstone and claystone, to coal beds, although many of the cycles are only partially preserved and are usually missing the fine grained units. Thicknesses vary considerably. Forty two measurements of the fining upward cycles average 4.2 m thick (corrected for a dip of 80° northward) with a standard deviation of 3.6 and maximum value of 19.3 m, whereas 260 measurements of individual units of conglomerate, sandstone, etc., average 1.4 m with a standard deviation of 1.5 and maximum value of 8.1 m (pebbly sandstone).

(d) Basaltic pyroclastites and epiclastites

Duke and Godwin (1986) described basaltic breccias, and ash to block tuff from exposures in Grew Creek. Some of the exposures are bedded.

A more than 250 m thick continuous sequence of basaltic ash tuffs, lapilli tuffs, and epiclastites is present in the drillholes at the western end of the Main Zone area and crops out northwest of the Main Zone. Units have considerable variability in thickness, up to a maximum of 37 m for lapilli tuff in section 9900E. Cyclic fining upward sequences are locally present, mostly in the epiclastites (see below), where the cycles resemble those in the fluvial sediments but are composed almost entirely of basaltic material.

The tuffs mostly consist of lapilli sized fragments (rare examples up to about 10 cm in diameter) and fine grained crystals (averaging 0.6 mm in diameter) of plagioclase and accessory quartz, in a fine grained ash matrix (Fig. 13). The lapilli are mostly basaltic, consisting of fine (0.3 mm) subhedral laths of plagioclase feldspar and lesser mafic minerals, and lithic fragments in a submicroscopic ash matrix (about 50%). Lapilli of a few units have been altered to pale hues of yellow, brown, green and red within the same rock, thus forming distinctive multicolored units compared to the pale green colour of most other altered rocks. A group of multicolored tuffs interbedded with basalt (flows?) forms a major marker unit in the western and central part of the Main Zone rhyolitic sequence (Fig. 5). Another set of units (not shown in Fig. 5) is present in the lower part of the eastern section, too low to be correlated with the upper unit, and is assumed to pinch out westward on the Grew Creek Fault.

(e) Basalt flows and dykes

Basalt flows and dykes are exposed in Grew and Rat creeks, and west of the Main Zone, and are intersected in the Main Zone drillholes (mostly logged by Noranda geologists as andesite).

In the Main Zone, the flows and dykes range from 0.1 to 38.7 m and average 4.5 m in intersection width downhole (the dips of the dykes are unknown). They are generally porphyritic with 5-30% phenocrysts (averaging 1-2 mm long but up to 10 mm) set in a microcrystalline (typically 0.5 mm) groundmass with some glass (0-20% but 40% in one sample). Weak glomeroporphyritic and variolitic textures are present in many samples, some are amygdaloidal (e.g. 72/135.3m) and one exhibits trachytic texture (83/62.5m).

Labradorite, some with oscillatory zoning, is the dominant phenocryst and microcrystalline phase, followed by clinopyroxene (zoned pale green diopsidic core to purplish titaniferous augite rim in sample 39/149.8m), opaques, and

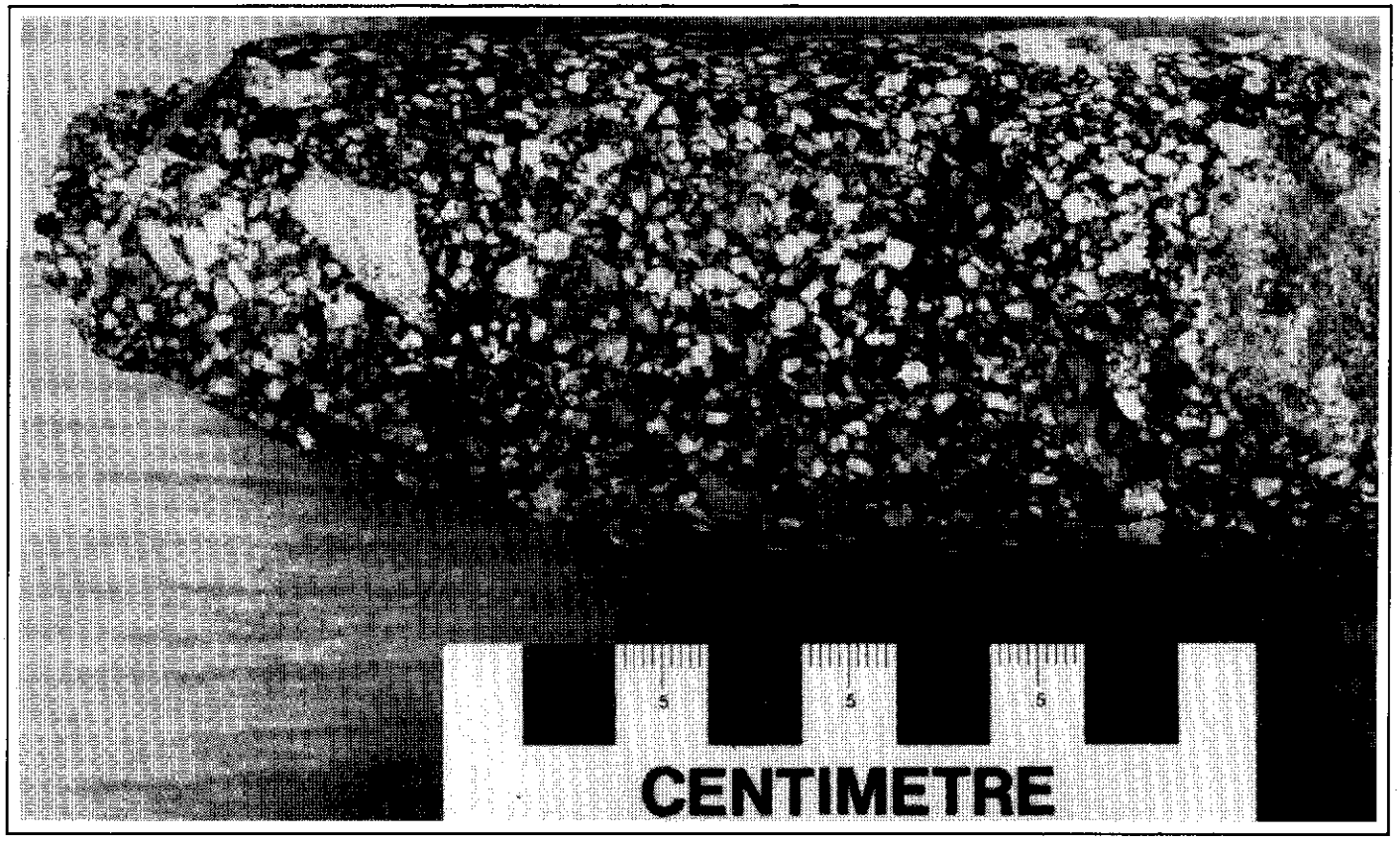

Figure 7. Drill core of S&P tuff from a downhole depth of 200.4 m in DDH 60.

Figure 8. Drill core of CLP tuff with 18 cm long pumice block (immediately above scale) at a downhole depth of about 72 m in DDH 72.

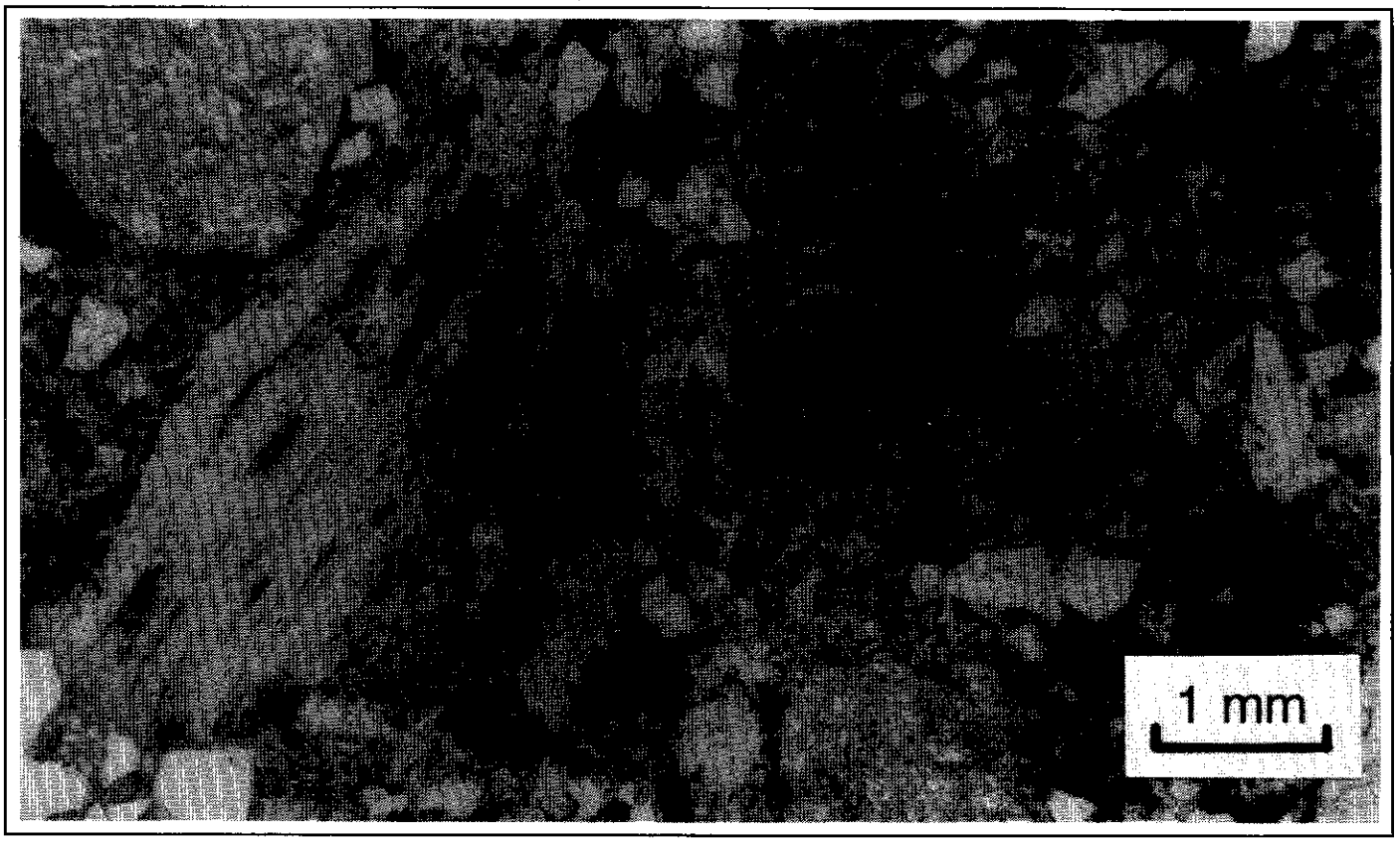

Figure 9. Thin section of CLP tuff (DDH 66 at 181.5 m downhole depth) under plane polarized light, showing quartz (white) and hydrothermally altered feldspar and rock fragments (mottled grey), pumice lower left) and pyrite (black).

Figure 10 Drill core of CLP tuff units (top and bottom) separated by a 40 cm thick (stratigraphic) trough cross bedded unit between 228.75 and 229.15 m downhole in DDH 69. At least three cross sets are present and may represent the basal surge layer of an ignimbrite sheet.

Figure 11. Drill core of welded vitric ash tuff from 123.3 m downhole in DDH 65. Mild eutaxitic texture is marked by partial flattening of pumice fragments (white).

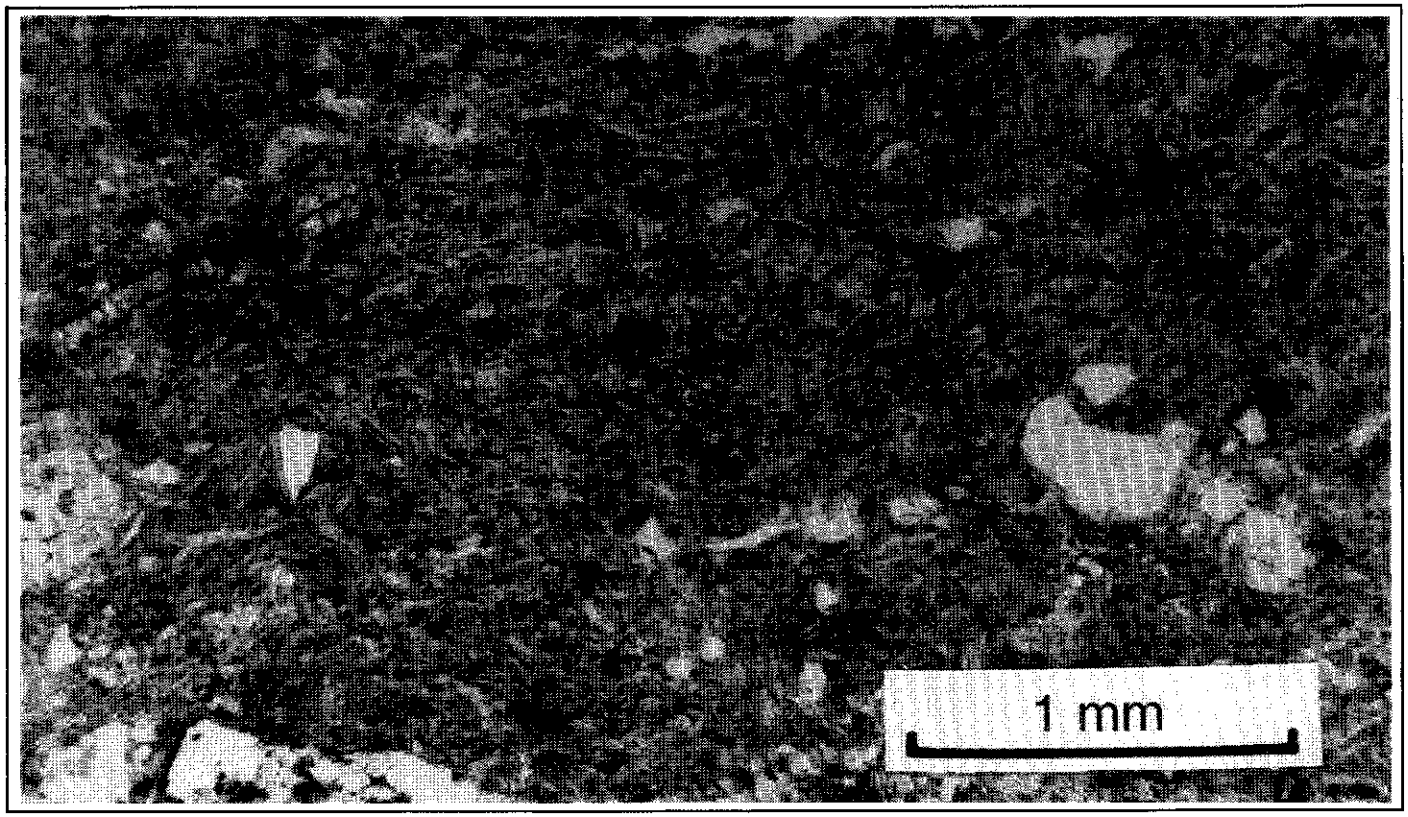

Figure 12. Thin section of vitric ash tuff (DDH 65 at 346.3 m downhole depth) showing sparse quartz fragments in a matrix dominated by glass shards (vitroclastic texture). Mild welding is marked by a preferred orientation of the shards.

Figure 13. Drill core of basaltic lapilli tuff from a downhole depth of 307 m in DDH 82.

Figure 14. Thin section of a medium grained diabase dike ("bird's foot porphyry") sampled at a downhole depth of 353.78 m in DDH 67. The rock consists of coarse subhedral plagioclase laths (altered to albite) with interstitial anhedral mafic (altered to carbonate and chlorite) and acicular opaque minerals.

olivine. Some labradorite and olivine phenocrysts have reaction and/or resorbed rims.

(f) Diabase (dolerite) dykes

Medium to coarse grained mafic dykes are exposed in Grew Creek and intersected in the drillholes in the Main and Tarn zones. Two rock types are identified:

1. Porphyritic rocks (e.g. 39/149.8m and 90/58.85m), which are essentially coarse grained basalts, with 10-30% plagioclase phenocrysts averaging 2-3 mm but commonly up to 7 mm long, and 5-10% mafic phenocrysts averaging 1 mm, clustered (glomeroporphyritic texture) or scattered in a 0.3-0.5 mm feldspar and mafic mineral groundmass. Needles of an opaque mineral (dendritic ilmenite?), averaging 0.3 mm long, make up about 5% of the rock.

2. Medium to coarse grained equigranular rocks (e.g. 67/353.78m and 90/44.7m; Fig. 14) which consist of 60-70% 1-1.5 mm (but up to 4 mm) plagioclase laths and 25-35% 0.5 mm mafic minerals. Needles of an opaque mineral, averaging 0.3 mm long, make up about 5% of the rock. We named these rocks "bird's foot porphyry" in hand specimen because of their variolitic texture. In thin section they are sub-ophitic and weakly variolitic. The original plagioclase composition could not be determined because of hydrothermal alteration to albite, illite and calcite but these rocks have almost identical chemical compositions to the basalts (see XRF geochemistry section below) and we therefore considered that they were diabase (dolerite). A similar but coarser grained rock (microgabbro) occurs as a dike crossing Grew Creek, near the camp.

HYDROTHERMAL ALTERATION

Introduction

Hudson Bay and Noranda geologists mapped hydrothermal alteration in the volcanic rocks south of the W-E Fault over a three kilometre strike length, including the Main and Tarn zones (Fig. 2B). The sedimentary rocks north of the fault are little altered apart from a few metres immediately adjacent to the fault in the Main Zone and north east of the Tarn Zone (Figs 2B and 4B). Alteration in the rhyolitic rocks is pervasive although there is some structural control on the intensity and type. The specific types of alteration present are listed below and in Table 2, and results of XRD analyses are listed in the Appendix:

1. Illite-quartz-adularia ± carbonate alteration is the predominant alteration type in the subsurface rhyolitic rocks. Other minerals which may be present include pyrite, interlayered illite/smectite, and albite. In the groundmass, felsic volcanic lithic fragments and pumice are generally altered to a finely crystallized mosaic of quartz and adularia. In moderate to strongly altered rocks, the lithics and groundmass textures merge into a recrystallized mass, and feldspar crystals are alterated to quartz, adularia, illite and carbonate.

2. Quartz-adularia alteration (silicification) occurs adjacent to some quartz veins and breccias including the discovery outcrop. It is gradational to illite-quartz-adularia ± carbonate alteration, representing an increase in the proportion of quartz and adularia.

3. Illite-quartz (sericitic or phyllic) alteration is represented by clay rich zones in the drillcore, particularly adjacent to veins, and brecciated, fractured or sheared zones. This alteration was logged by Noranda as argillic because of the presence of clays in hand specimen. The primary clays are predominantly illite, with lesser interlayered illite/smectite and smectite, overprinted with secondary kaolinite and therefore we prefer to classify this alteration as illite-quartz and not argillic. Illite-quartz alteration is gradational with illite-quartz-adularia ± carbonate alteration, representing an increase in the proportion of illite and quartz.

4. Carbonate-chlorite (propylitic) alteration is the dominant alteration type in basaltic rocks. Other minerals that may be present include albite, illite, quartz, pyrite, adularia, interlayered illite/smectite, and interlayered chlorite/clay (-illite?). The alteration of mafic minerals, and to a lesser extent feldspars, is dominated by the development of the carbonates calcite, siderite and dolomite, which form pseudomorphs of the original minerals and fill voids and vesicles. Alteration of feldspars has also produced illite, K-feldspar and quartz, whereas chlorite and pyrite have replaced the mafic minerals. XRD analyses also indicate the presence of minor smectite, interlayered illite/smectite and chlorite/smectite (Appendix). Epidote was noted in one hand specimen of drill core. Amygdules are filled with calcite, sometimes with a chalcedonic quartz core.

5. Intermediate argillic alteration was mapped by Duke and Godwin (1986) in the rhyolitic rocks exposed in surface trenches within the Main Zone and it is also present, particularly as an overprint clay assemblage, in some subsurface zones. It is characterized by abundant smectite and may also contain kaolinite, pyrite, interlayered illite/smectite, quartz and relict carbonate, illite and K-feldspar. The relict minerals in some of the trench material indicate that alteration of this material may have been primarily illite-quartz-adularia ± carbonate type, later overprinted by argillic alteration.

6. Advanced argillic (acid sulphate) alteration is clay alteration characterized by the presence of alunite and/or abundant kaolinite, and was identified by Duke and Godwin (1986) in rhyolitic rocks in the trenches in the Main Zone. Other minerals which may be present include smectite, quartz, pyrite, and relict carbonate and interlayered illite/smectite.

7. Weathering: Much of the strong "argillic" clay alteration, in both the illite-quartz-adularia+/-carbonate and propylitic alteration zones, may result from supergene alteration by surface weathering and/or acidified (from the oxidation of pyrite) groundwater. Duke and Godwin (1986) noted a deep weathering profile with a clay-carbonate mineral assemblage at Grew Creek. We were impressed at the rapid rate that rocks in exposed trenches and drill core decomposed to clay. Post-drilling weathering and resultant clay alteration was particularly noticeable in drill core when a complete hole was laid out. In many of the early holes, we noted that every tenth core box was extensively clay altered. This was because the core trays had been stacked in open racks, ten trays high and the rock in the exposed top tray was weathering more quickly than that in the other trays. The core tray racks were roofed subsequent to our work. Strong clay alteration elsewhere was generally concentrated near faults or sheared and crushed zones, and could be attributed to either late hydrothermal or supergene processes.

Alteration trends

We plotted hydrothermal alteration and visually estimated pyrite concentrations from the Noranda lithological drill logs for several cross-sections (listed as coordinates in Fig. 3), and correlated this data with our logs and analytical results to determine the alteration pattern and trends.

The hydrothermal alteration forms an envelope around the mineralized zone. The complete drill tested width of the Main Zone (about 300 m) is altered, but medium to high intensity alteration is concentrated within a width of about 100 m. Basaltic rocks within the rhyolitic sequence are altered to carbonate-chlorite (propylitic) assemblages, whereas those to the west, faulted against the rhyolitic sequence, are little altered (although green in hand specimen). At the time of alteration, they may have been remote from the centre of hydrothermal activity, but later, may have moved close to the mineralization along the intervening fault. Illite-quartz-adularia+/-carbonate alteration is the most common type of alteration in the rhyolitic sequence. This grades into illite-quartz, argillic (overprint?), or quartz-adularia alteration around major veins and other fracture structures. Quartz-adularia is the highest rank of alteration present and is usually associated with zones of quartz veining but not necessarily vice versa. Although quartz-adularia alteration is present up to the highest level in some drillhole cross-sections, in many others it passes upward into illite-quartz and illite-quartz-adularia$\pm$carbonate alteration with similar (and sometimes greater) frequency of quartz veining (Fig. 4B). Illite-quartz and argillic clay zones associated with structural features range in thickness from a few centimetres to several metres. This clay alteration is considered the primary reason for poor recovery in mineralized intersections (c.f. Duke, 1988; Seto and Crowe, 1989).

Welded and partly welded CLP units present at various horizons are consistently moderately to intensely altered to illite-quartz-adularia and illite-quartz assemblages, suggesting that this lithology was highly permeable and thus more susceptible to alteration. As a highly competent rock, it would have developed good fracture controlled permeability. Following alteration, the permeability would have been greatly decreased, thus causing the uppermost partly welded CLP unit adjacent to the W-E Fault to act as an aquiclude to hydrothermal fluid flow. Where this unit is present, the fluvial sediments across the W-E Fault are little altered, whereas where it is absent, the sedimentary rocks exhibit much greater alteration, extending more than 100 m into the sedimentary sequence on section 10050E.

Intermediate argillic and advanced argillic alteration are the main types of alteration in the upper parts of the system mostly as an overprint on earlier illite-quartz-adularia$\pm$carbonate alteration.

The concentration of pyrite shows poor correlation with intensity of alteration, veining, and mineralization but exhibits a strong increase in concentration in the vicinity of the W-E Fault, and particularly in the adjacent partly welded CLP unit (Fig. 15). This results in a pyrite zone adjacent to and north of the mineralization.

MINERALIZATION

Gold and silver mineralization of the Main Zone occurs in stockwork quartz veins and hydrothermal breccias. The quartz veins are mostly 2-10 cm but possibly up to 1 m thick, and the hydrothermal breccias are a few centimetres to 1 or 2 m thick. Many of the quartz veins are banded on a millimetre scale and some consist of, or contain bands of, brecciated and recemented vein material. The larger veins and breccias are poorly preserved in the drill core because of their broken nature and resultant poor core recovery (Noranda drill logs). Rubbly vein and breccia material, logged up to maxima of about 5 m and 10 m of apparent drill core length respectively, are not considered true representations of original widths of the veins and breccias because part of these drill lengths would have been occupied originally by clay altered wall rocks that have been flushed away during drilling.

Plots for some drill cross-sections showing veins noted in the Noranda drill logs (Fig. 3) indicate that veining is mostly confined to a steeply northward dipping zone, 40 m to 80 m wide. The veins die out below the 650 m elevation on most sections but extend down to at least the 550 m elevation on sections 10150E and 10200E (the intervening 10175E section was not plotted), suggesting a funnelling down in this area. The greatest density of veins per unit distance occurs at intermediate depths.

Stroshein (1986a) considered that the discovery outcrop was a hydrothermal vent breccia. This outcrop is severely weathered and although it exhibits clast textures, we consider it is more likely to be quartz-adularia altered coarse CLP tuff, part of which projects to this surface position on the stratigraphic section (Fig. 5).

The main non-metallic phases in veins and hydrothermal breccias are quartz, adularia, carbonates, clays (mostly illite), and quartz pseudomorphous after calcite. Additionally,

fluorite occurs in the Tarn Zone veins. The quartz is mostly chalcedonic and rarely finely crystalline. Crystal lined vugs are very rare.

McNeal (in Duke, 1988) noted that pyrite and marcasite are the main metallic minerals but there are also traces of arsenopyrite, chalcopyrite, sphalerite, galena, electrum, acanthite, naumannite, aguilarite, and silver amalgam. The electrum averages 7.5 μm in diameter, with a maximum diameter of 60 μm. Eleven analyses range in fineness from 640 to 160 and average 360 fine (64 to 16 and 36 weight percent Au respectively).

GEOCHEMISTRY

XRF and ICP analyses

Whole-rock XRF (X-ray fluorescence) and ICP (Inductively Coupled Plasma Spectroscopy) analyses of samples of basaltic and rhyolitic rocks are presented in the Appendix. When normalized free of water and carbon dioxide (Table 3), the analyses of basalt and rhyolite are similar to those from Grew Creek and nearby occurrences previously reported by Duke and Godwin (1986), Jackson et al. (1986), and Pride (1988). Jackson et al. (1986) concluded that the basalts were calc-alkaline to transitional tholeiites, whereas the rhyolites were a high potassic subaluminous type.

Measurements of rock density were made and the analyses converted to units of kg/m^3 to reduce the apparent enrichment and depletion effects caused by changes in rock density during hydrothermal alteration. Densities were measured with a Walkers Steelyard beam balance and used in the following formula:

$$\frac{Wt\%}{\sum -H_2O-CO_2} \times \rho = \frac{kg}{m^3}$$

Where Wt% = weight percent of oxide = ppm x 10^{-4}

ppm = parts per million of element

Σ = total of analysis (Wt%)

H_2O = water loss on drying (Wt%)

CO_2 = carbon dioxide (Wt%) determined by wet chemical methods

ρ = density in kg/m^3

Binary plots of oxides and elements versus silica, presented in Figs 16 and 17, were constructed using the density corrected data in the computer program IGPET-II from Terra Soft Incorporated, New Jersey. Even though hydrothermally altered, the different rock types form distinct trends and groupings on these plots, generally with the tuffs lying between basalt and rhyolite end members in the order: basalt, basaltic tuff, S&P tuff, CLP tuff, VT tuff, and rhyolite. The intermediate composition of the tuffs reflects the presence of both basalt and rhyolite pyroclastic fragments. Separation of the various rock types is particularly good in binary and ternary plots (not shown) using Cr, Co, Cu, Ni, Y, La, and Pb.

Basaltic rocks: All of the basalt samples are propylitically altered, with intensities of alteration ranging from mild (55/30.7m) to strong (72/117.6m and 66-115.2m). This is reflected in their high loss on ignition (H_2O, CO_2 and S) in comparison to average analyses of basalts from exposures in Grew Creek and other nearby occurrences reported by previous authors (Table 3). Also, our hydrothermally altered basalts exhibit a marked K_2O enrichment, and are slightly enriched in Al_2O_3 and Na_2O (probably secondary illite, K-feldspar and albite), in addition to carbonate. In contrast, within our suite of analyses, trends exhibited with increasing intensity of alteration are generally in reverse to those mentioned, although at subdued levels: there are small decreases in K_2O, Na_2O, SiO_2, and Al_2O_3, a small increase in CaO, and possibly a slight increase in MgO (probably reflecting an increasing importance of secondary carbonate and chlorite).

Rhyolitic rocks: The rhyolites analysed are all similarly moderately altered to illite-quartz-adularia$\pm$carbonate assemblages, although sample 90/98.6m is more strongly altered and close to an illite-quartz assemblage. This sample is distinguished from the others by having greater Na_2O and less TiO_2, CaO and Al_2O_3. However, in comparison to less altered rhyolites reported from other nearby occurrences by previous authors, the Grew Creek rhyolites are depleted in Na_2O (Table 3). An initial assessment of the suite of tuff samples indicates that the markedly different chemistry of the individual tuff types (S&P, CLP, and VA tuffs) may mask the alteration effects, but further work is in progress.

Drill core assays

Noranda sampled a half split of the drill core over intervals of 1.5 m in holes DDH 19 to DDH 90 but used a smaller sampling interval (e.g. 0.5 m or 0.75 m) over all or parts of DDH 14 to DDH 18. Similarly, Hudson Bay sampled DDH 1 - DDH 13 using varying intervals (mostly between 0.5 m to 1.5 m). All Hudson Bay core samples were analysed for gold by fire assay, silver by hot HCl-HNO_3 extraction and atomic absorption, arsenic by perchloric-HNO_3 extraction and colorimetry, and mercury by flameless atomic absorption. Noranda core samples were analysed for gold and silver by fire assay, iron and arsenic by hot HCl-HNO_3 extraction and ICP, and mercury by flameless atomic absorption. Composite 5 m samples of holes 29 and 30 were analysed for a suite of 30 elements by hot acid extraction and ICP (Table 4). The composite sample ICP analyses are useful for comparative purposes, however they may underestimate the real concentrations of many elements by about 50% - 75% (c.f. Sketchley, 1985), because of only partial leaching of the

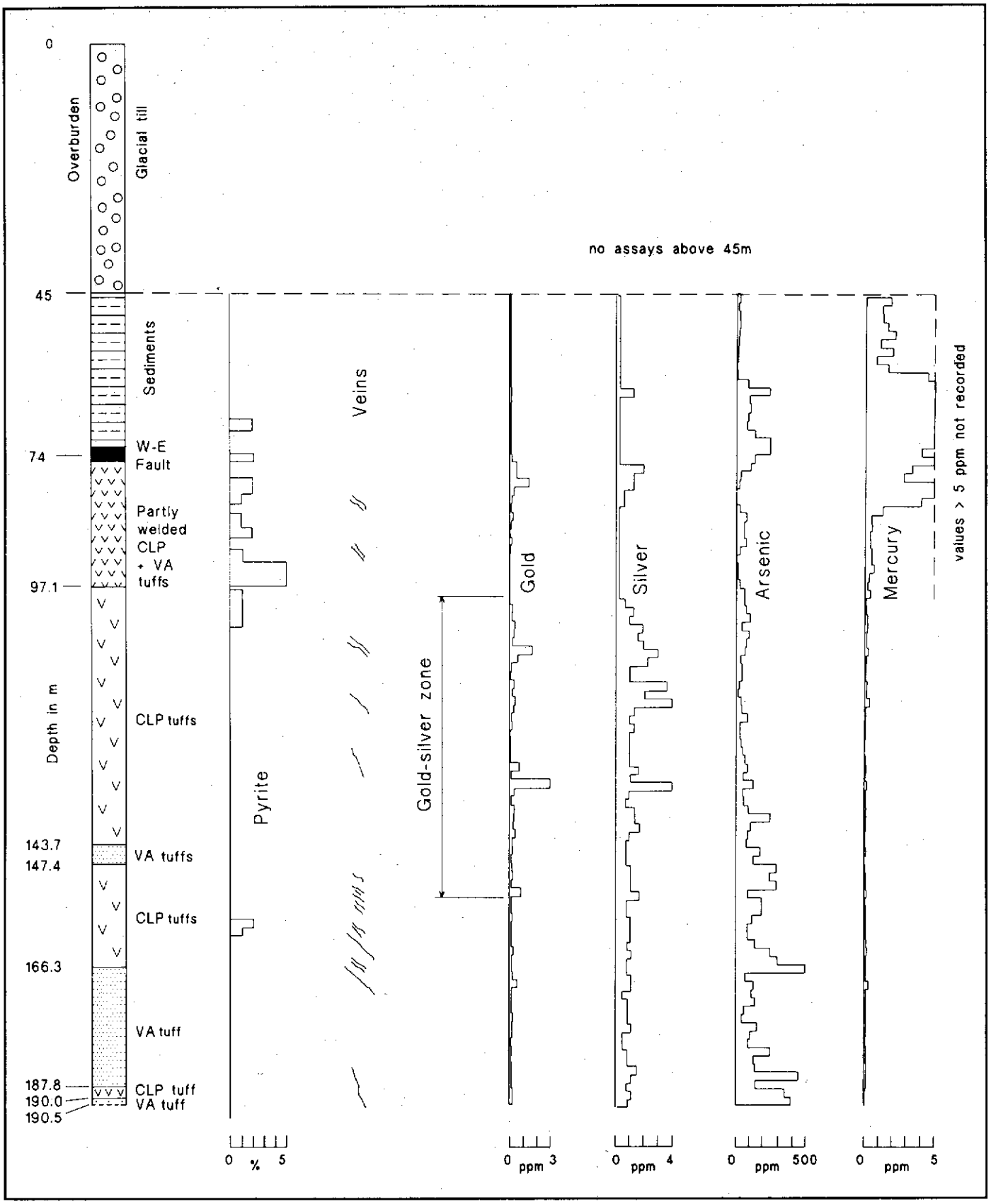

Figure 15. Down hole trends in DDH 34 (190.5 m diamond drillhole, section 10150E, bearing 199°, and dipping 45°; see Figure 3).

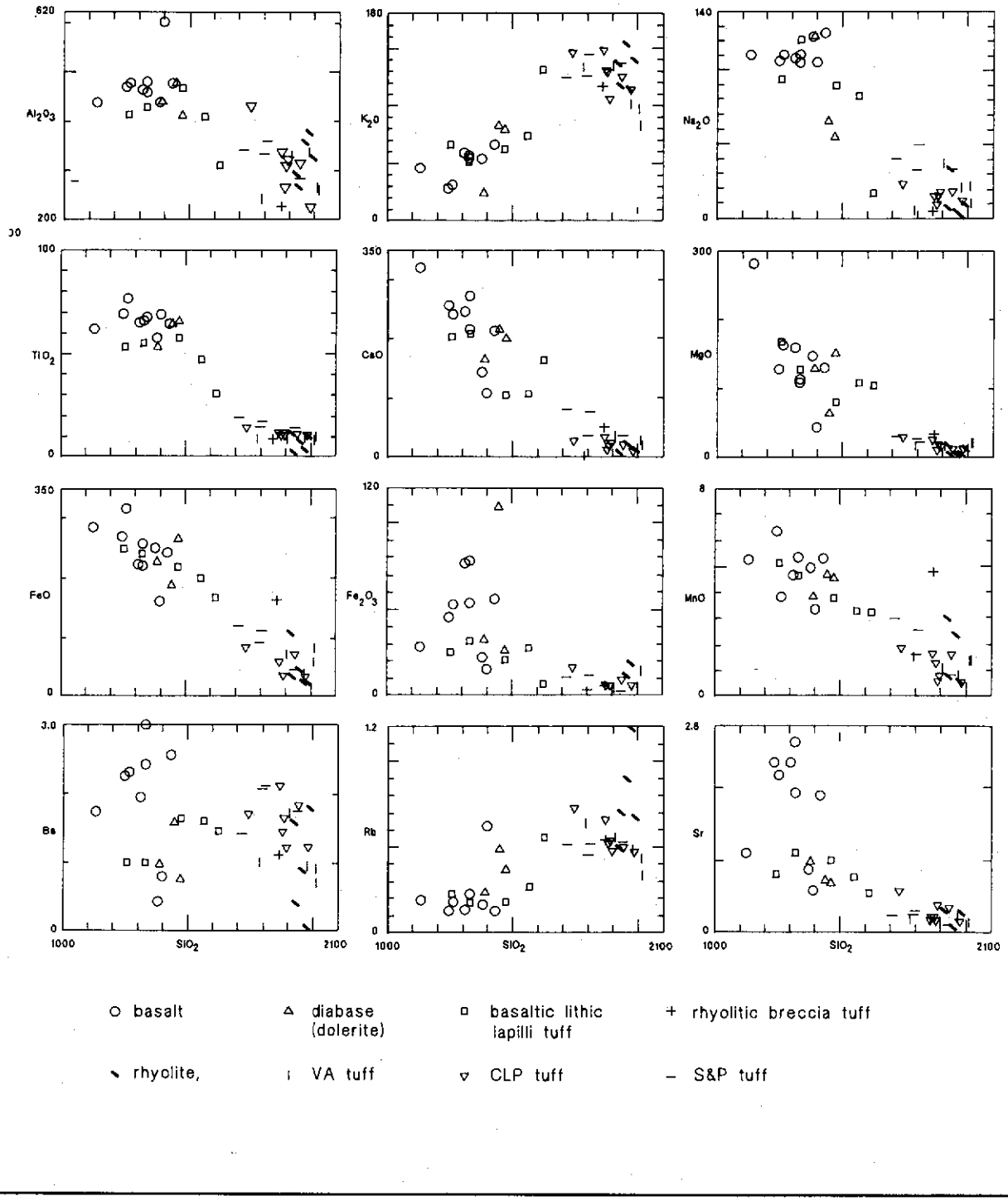

Figure 16. Binary plots for whole-rock XRF and ICP analyses against SiO_2 corrected for density. Units are kg/m^3. The analyses show positive variations of K_2O and Rb and negative variations of all other oxides and elements except Ba which exhibits an almost buckshot pattern.

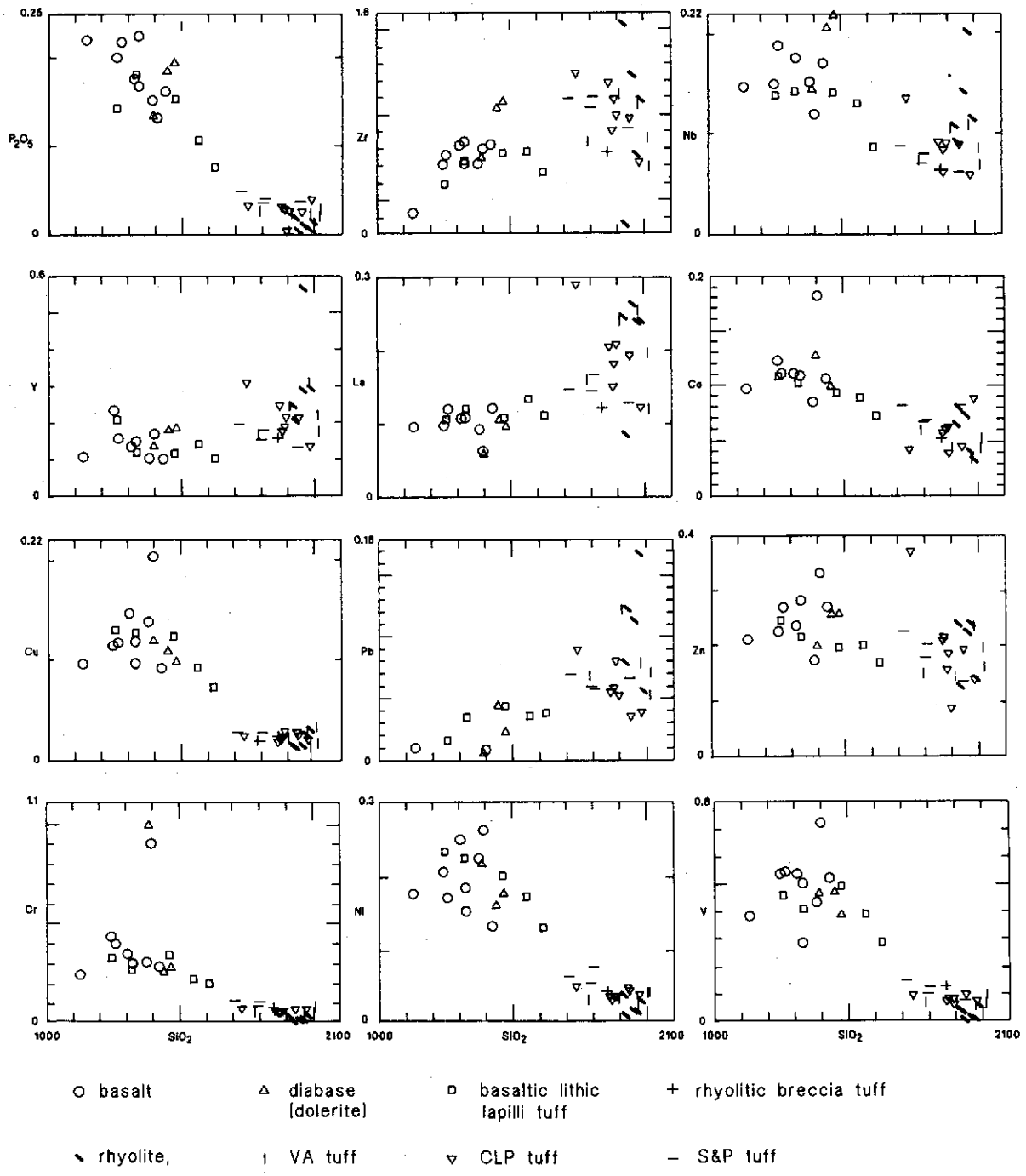

Figure 17. Binary plots for whole-rock XRF and ICP analyses corrected for density. Units are kg/m^3. The analyses form positive (Zr, Y, La, and Pb) and negative (all others) variation trends with SiO_2.

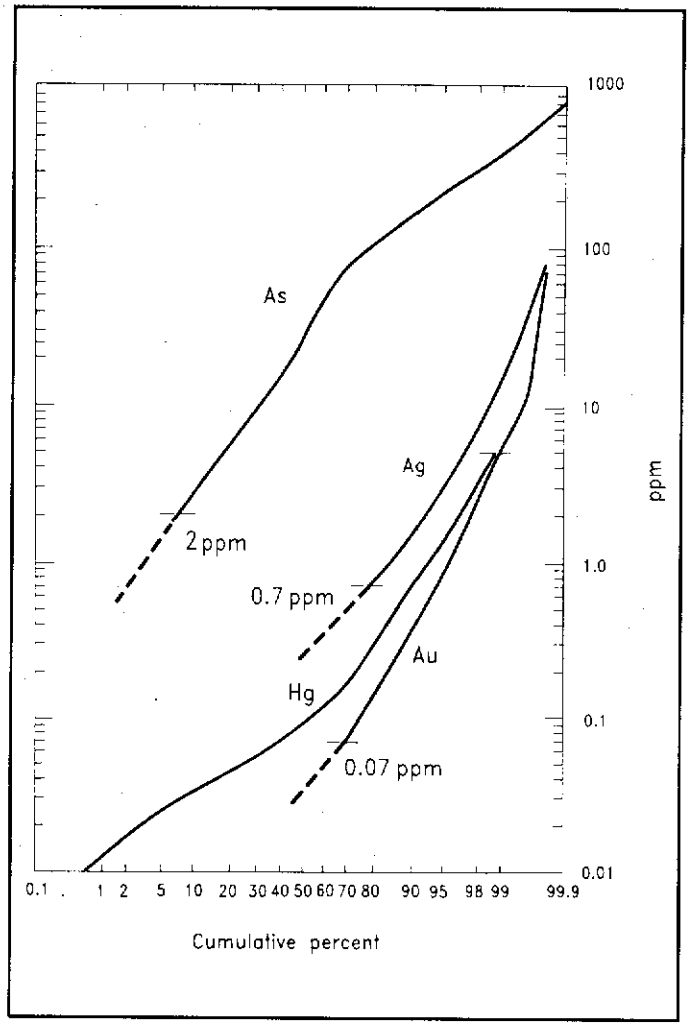

Figure 18. Cumulative probability curves of As, Ag, Hg, and Au for 11,416 samples from DDH 1 to DDH 90 but excluding holes DDH 17 and DDH 65 (analyses not available). As, Ag and Au are truncated at their lower ends by detection limits of 2 ppm, 0.7 ppm and 0.07 ppm respectively. Hg is truncated at the upper end by a maximum recorded assay level of 5 ppm for some Hg-rich samples. Statistical parameters are listed in Table 5.

elements during extraction. Nevertheless, concentrations for silver determined by the two different analytical techniques showed good agreement, although many of the low concentration values are below the ICP detection limit and the high concentration values generally have higher peak values in the ICP analyses.

The various analyses show that, in addition to gold and silver, the mineralization exhibits strongly anomalous arsenic and mercury concentrations, but low concentrations of copper, lead, zinc, antimony and barium, and very low concentrations of molybdenum, nickel, cobalt and tungsten (some shown in Table 4 and Fig. 15). Uranium and thorium were below their analytical detection limits.

Cumulative probability plots for 11,416 drillhole assays of gold, silver, arsenic and mercury are shown in Fig. 18 and some statistics generated using the MINITAB computer program (MINITAB Incorporated, Pennsylvania State University) are listed in Table 5. About 70 % of gold and 80% of silver values are below the detection limits for these elements (0.07 ppm for Au and 0.7 ppm for Ag). At 1 ppm gold (96th percentile), equivalent concentrations of other elements are: 3.4 ppm silver, 235 ppm arsenic and 1.54 ppm (1540 ppb) mercury.

Regression lines and R-squared values for correlation between gold, silver, arsenic, and mercury assays were calculated using MINITAB and are shown in Fig. 19; the regression equations are listed in Table 6. The arsenic-mercury pair was calculated using assays for all 11,416 samples, whereas gold-silver, gold-arsenic, gold-mercury, silver-arsenic, and silver-mercury pairs were calculated using assays of a subset of 2,771 samples with gold greater than 0.07 ppm and silver greater than 0.7 ppm (i.e. above their detection limits). There is relatively good correlation between gold and silver (R-sq = 50.6%), weak correlation of silver and mercury (R-sq = 18.0%) and gold and mercury (R-sq = 14.6%), and little correlation between mercury and arsenic (R-sq = 2.4%). There is no correlation between gold and arsenic or silver and arsenic (R-sq = 0.1% each). The gold-silver regression line shows a decreasing gold:silver ratio with increasing concentration, e.g. 1:3 at 1 ppm gold and 1:6 at 3 ppm gold.

Visual examination of computer plotted drill sections, showing downhole assays as histograms, for 12 cross-sections (listed as coordinates in Fig. 3) confirms the statistical analysis. Gold and silver show strong correlation and their enrichment in many of the sections defines a steeply northward-dipping gold-silver mineralized zone (termed the Gold-silver Zone) within the rhyolitic tuffs, southward and below the W-E Fault and upper welded CLP unit (Figs 2A, 4C, 15, and 20). In contrast, mercury exhibits a strong enrichment above and north of the Gold-silver Zone in the vicinity of the W-E Fault, with enrichment in the adjacent rhyolitic tuffs and fluvial sediments, defining a mercury zone partly coincident with the pyrite zone (Fig. 15). In some holes, a second order enrichment of mercury associated with the Gold-silver Zone, has caused the weak correlation with gold and silver suggested by the statistical analysis. A local third order enrichment of mercury is associated with some breccia zones, faults other than the W-E Fault, and lithological contacts in a few holes. Arsenic shows elevated concentrations throughout large sections of the drillholes, and exhibits some local correlations with elevated gold and silver and/or mercury, but there is no consistent trend (e.g. Fig. 15).

Down hole trends in the southward angled holes 29 and 30 are illustrated in Fig. 20, from analyses listed in Table 4. There are coincident high concentrations of gold and silver representing the Gold-silver Zone, half to two thirds of the way down the holes. Lead and zinc are depressed around the

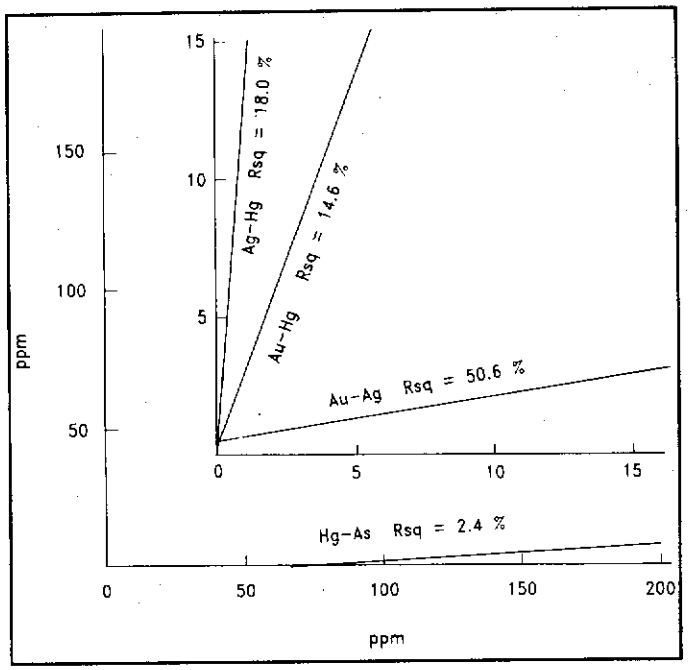

Figure 19. Plots of regression lines determined for drill core assay data (see Table 6). The vertical axis scale relates to the first element listed in each element pair, whereas the horizontal scale relates to the second element.

Gold-silver Zone and show strongest concentrations higher in the holes (north of the Gold-silver Zone). Copper values are high in the Gold-silver Zone and similar copper values occur uphole with lead and zinc in DDH 30. Antimony values are highest near the top of the holes but also show a lesser concentration in the Gold-silver Zone. Cobalt and nickel generally follow iron with concentrations in the upper parts of the hole, above the Gold-silver Zone, and a narrow peak near the bottom of each hole. Manganese also generally follows iron but has an irregular pattern in the upper part of DDH 30. Arsenic has an irregular distribution, but shows small peaks in the Gold-silver Zone.

The Gold-silver Zone occurs in the shape of an elongated wedge, widening upwards, and has approximate maximum dimensions of 550 m long, 110 m wide and 150 m deep. The east end of the zone is defined by a marked decrease in grade, whereas the western end is faulted off against the basaltic rocks. The highest gold values lie between the vertical cross-sections 10150E and 10350E, and above the 700 m level horizontal section, with a rapid decrease in gold grade away from this zone. Grade in the Gold-silver Zone appears to increase upward to the point where the zone is truncated by erosion. The only high level part of the system which is preserved is the discovery outcrop, which assays fairly low levels of gold and silver. However, this does not necessarily indicate an overall fall-off of Au-Ag at this level because the outcrop is about 100 m to the west of the high grade zone. A feeder zone may be present near section 10200E where high assays extend down to a level of almost 700 m and quartz veining also appears to funnel down (see Mineralization section). In other sections, drillholes below the high grade zone return low gold assays. The possible extension of high grade gold values below 700 m in section 10200E was not drill tested.

DISCUSSION

Volcanic environment

Contemporaneous basaltic and rhyolitic volcanism is indicated by: (1) interbedded basaltic tuffs and flows in the rhyolitic sequence, (2) fragments of basalt in the rhyolitic tuffs, and (3) abundant quartz xenocrysts in some of the basaltic tuffs. The Tarn Zone rhyolites are considered to represent a rhyolite dome which, by reason of proximity, was probably the source of the rhyolitic pyroclastic rocks in the Grew Creek area, although there are other potential source rhyolite domes within a few kilometres distance (see Gordey and Irwin, 1987).

A basaltic eruptive centre west of the Main Zone is suggested by the predominance of basaltic rocks at the western end of the Main Zone, and strong magnetic anomalies extending to the west.

The CLP and VA tuff units are considered to have been erupted as a series of ignimbrites (ash flow tuffs). The high crystal and lithic fragment content and degree of sorting of the S&P tuffs suggests a high degree of initial fragmentation of a crystal rich magma and/or efficient sorting processes during eruption and transport (see review of possible origins of crystal rich tuffs by Cas, 1983). Crystal-lithic rich ignimbrites similar to the S&P tuffs have been described elsewhere, for example Victoria, Australia (Birch, 1978; Clemens and Wall, 1984) and Colorado (Lipman, 1975), and therefore an ignimbritic origin is also possible for the S&P tuffs. The individual S&P units are generally homogeneous and lack sedimentary structures or other features which might help further determine their origin.

Sedimentary environment

Hughes and Long (1980) and Long (1981) described Tertiary age, coal bearing fresh water clastic sediments from many localities within the Tintina Trench and suggested that they resulted from sedimentation within separate orinterconnected fault controlled basins. Cyclic fining upward sequences at a few locations were considered to indicate deposition in river, deltaic (fine sequences) and alluvial fan (e.g. coarse sequences at Lapie River and Watson Lake) environments. The Grew Creek cyclic fining upward sequences are similar to point bar deposits formed by meandering streams, but the abundance of conglomerates suggests that an alluvial fan environment may have been more likely. During tectonically active episodes, alluvial fans would be common within the Tintina Trench, receiving detritus from the rapidly eroding marginal fault scarps.

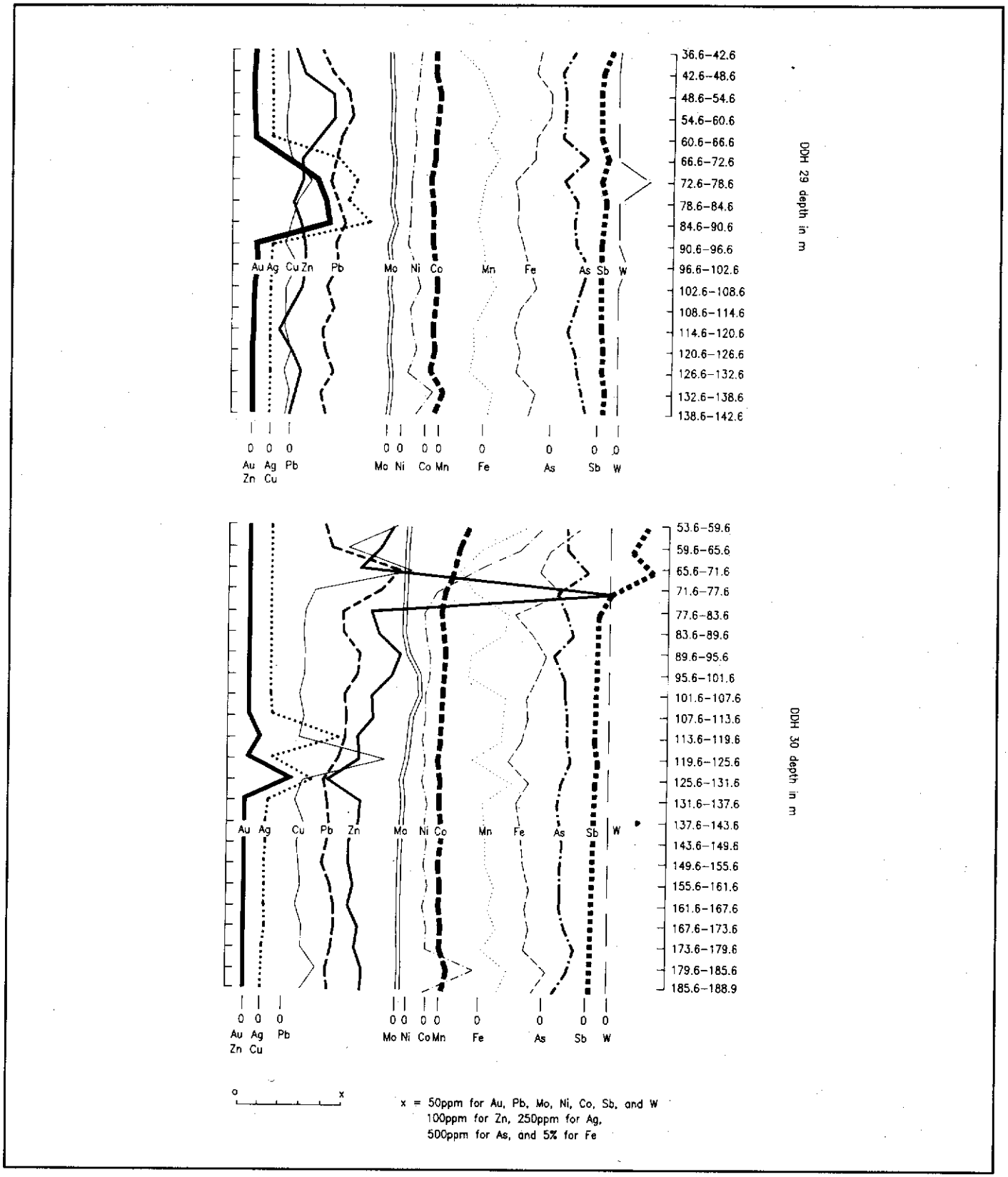

Figure 20. Downhole trends for concentrations of several elements determined by ICP analyses of 6 m composite samples (Table 4), together with Au and Ag curves based on averages of fire assays for 1.5 m samples. Au and Ag exhibit strong concentrations half way (DDH 29) to two thirds (DDH 30) downhole depth, defining the Gold-silver Zone, whereas Pb and Zn exhibit concentration peaks higher in the holes. Cu peaks in both zones in DDH 30.

Hydrothermal environment

The Grew Creek hydrothermal system exhibits many of the well documented features of volcanic hosted, low sulphur, quartz-adularia, epithermal and geothermal systems (see Berger and Eimon, 1983; Bonham, 1986; Hayba et al., 1986; Henley, 1986). The widespread illite-quartz-adularia alteration in the permeable tuffs, and propylitic alteration of the basaltic rocks, are typical of equilibration with near neutral pH alkali chloride water. The presence of illite and trace epidote suggests temperatures of $>220°<250°$ C. The quartz-adularia alteration results from high permeability in the tuffs and adjacent structurally controlled channelways (now veins and breccia zones), accompanied by higher fluid temperatures, and a more alkaline pH, probably produced by boiling. Cyclic sealing of channelways by mineral deposition and subsequent rupture by overpressure and hydraulic fracturing produced the hydrothermal breccias and ruptured veins. Intermediate argillic and advanced argillic alteration of the near surface rocks resulted from equilibration with acid sulphate water, evolved from the alkali chloride water by oxidation of contained sulphide to sulphate, or condensation in near surface waters of H_2S and CO_2 evolved from boiling.

Structural and stratigraphic control of mineralization

The mineralization is structurally controlled on all scales. The deposit occurs along splinter faults of the Tintina Fault Zone, and is localized where these are intersected by the second order, northerly striking N-S Fault. These features were probably the control for focusing deep fluid upflow at Grew Creek. Nearer surface, high permeability was provided by the rhyolitic tuffs (primary permeability) and numerous small scale tensional faults and fractures, now represented by veins and breccia zones (secondary permeability). The high primary permeability of the rhyolitic tuffs was probably a key factor in the development of the stockwork vein and breccia style of mineralization. Alteration and sealing of the upper welded CLP unit, accompanied by strong pyrite enrichment, prevented flow of hydrothermal fluid into the clastic sediments and confined the mineralization mostly in the non-welded CLP units. Mercury was concentrated along the W-E Fault possibly sometime after mineralization.

Tectonic style

The Grew Creek area records several local changes of tectonic style within a short period. Bimodal basalt-rhyolite volcanism, by analogy with similar occurrences elsewhere, was probably associated with regional extension. The mineralization occurs in approximate original orientation (near vertical veining), whereas the host rocks dip steeply, indicating that most of their tilting, as a result of a compressional tectonic regime, was pre-mineralization. Subsequently, mineralization was probably associated with extension because quartz veins are generally dilatant structures. However, the Grew Creek stockwork vein and breccia structures were generated by the hydrothermal system itself, i.e. by hydrofracture mechanisms, which could develop in either a compressional or extensional environment.

Sequence of events

The sequence of events at Grew Creek is considered to be as follows:

1. Around 60-50 Ma, a local tensional tectonic regime within the Tintina Fault Zone caused the formation of a pull-apart basin and associated bimodal basalt-rhyolite volcanism. Clastic sediments were also deposited within the basin.

2. A period of local compressional tectonics caused major deformation of the rocks including tilting and folding.

3. Around 50 Ma, a hydrothermal system developed, probably within a local extensional tectonic environment. Deep fluid upflow was localised at the intersection of the Grew Creek, North-South, and West-East faults. Near the surface, the hydrothermal fluid flowed into and through the permeable nonwelded ignimbrites, causing hydrothermal alteration and mineral deposition in these and adjacent units, including the formation of the pyrite zone. This was followed by the development of a hot springs style epithermal deposit with cyclic sealing and rupture resulting in quartz veining and hydrothermal breccias.

4. Cessation of hydrothermal activity was followed by additional faulting with considerable crushing and breaking of the veins and immediately adjacent wall rocks. This provided good secondary permeability for penetration and circulation of groundwater through the deposit, causing substantial supergene clay alteration. Considerable movement along some faults is demonstrated by the juxtaposition of the moderately to strongly altered rocks of the Main Zone against the little altered basaltic rocks in the west.

SUMMARY AND CONCLUSIONS

1. The Grew Creek prospect is a volcanic-associated epithermal gold-silver deposit of the low sulphur, quartz-adularia type.

2. The "Main Zone" deposit is hosted by rhyolitic tuffs, grouped into: (1) "crystal-lithic rich" mixed coarse ash tuff, lapilli-ash tuff, and lapilli tuff, (2) "glass rich" mixed coarse ash tuff and lapilli-ash tuff, and (3) vitric ash tuff. Welding and hydrothermal alteration have given some tuff units a pseudo rhyolite or quartz-feldspar porphyry appearance in hand specimen, causing previous misidentification of these rocks. The tuffs were most probably erupted as a series of ignimbrite (ash flow tuff) sheets associated with a rhyolite dome in the "Tarn Zone", 4 km to the east-southeast. The rhyolitic rocks are faulted against basaltic pyroclastic rocks

and flows to the west and fluvial sediments to the north.

3. An alkali chloride-type hydrothermal fluid altered the rhyolitic rocks adjacent to the veins to quartz-adularia and illite-quartz assemblages, and elsewhere to illite-quartz-adularia ± carbonate assemblages. Basaltic rocks are altered to carbonate-chlorite assemblages. Acid sulphate fluid formed intermediate argillic and advanced argillic alteration in the near surface environment. Hydrothermal alteration of the sediments is limited to a zone adjacent to the W-E Fault.

4. Gold and silver mineralization occurs in stockwork veins and hydrothermal breccias. The major minerals are electrum and acanthite, with associated pyrite, marcasite, and traces of arsenopyrite, chalcopyrite, sphalerite, galena, naumannite, aguilarite, and silver amalgam, in a gangue of quartz, adularia, carbonates, clays (mostly illite), and quartz pseudomorphous after calcite. A localized concentration of pyrite above and north of the mineralization forms a pyrite zone.

5. The mineralization occurs in a zone shaped like an elongate wedge, widening upwards, approximately 550 m long, 110 m wide and 150 m deep. The eastern end of the zone is defined by a marked decrease in grade, whereas the western end is faulted off against the basaltic rocks. Within the zone, the highest gold and silver assays occupy a level lying above the most intense quartz veining. Gold concentrations vary proportionally with silver, generally in a 1:4 ratio in the ore grade mineralization. A zone of anomalous mercury geochemistry is associated with the W-E Fault and coincides with the pyrite zone. Arsenic is present in anomalous concentrations but there is no statistical correlation with gold and silver when viewed in detail.

6. Hydrothermal activity and mineralization were intimately linked with the tectonic environment of the Tintina Fault and suggest a major period of activity along the fault in the mid Eocene. The deposit is hosted by volcanic rocks formed during extension in a pull-apart basin along the Tintina Fault Zone. Episodic fault movements structurally prepared the Grew Creek area by providing locally high secondary permeability for the focus of upflowing hydrothermal fluids.

7. The high primary permeability of the rhyolitic tuffs resulted in the development of mineralization structures by hydrofracture type mechanisms, producing the stockwork vein and breccia style of mineralization.

8. The absence of significant mineralization and hydrothermal alteration in the clastic sediments is attributed to damming of the hydrothermal fluids by the partly welded tuffs along the footwall of the W-E Fault.

9. Mineralization postdated tilting of the sedimentary and pyroclastic sequences.

10. Post-mineralization movements along the Tintina Fault Zone have disrupted the deposit, with displacements along several parallel and oblique faults, and crushing of vein material and adjacent wall rocks.

ACKNOWLEDGEMENTS

Christie carried out research on this project while on study leave from New Zealand Geological Survey (now DSIR Geology and Geophysics), and was hosted by Geological Survey of Canada in affiliation with the Department of Geological Sciences, University of British Columbia. These organizations are thanked for their support. Ken Dawson and Jim Morin suggested the topic. Fieldwork by Christie and Rushton, and some direct project costs were funded by a research grant from Indian and Northern Affairs Canada and supported by Noranda and Golden Nevada. Steve Morison, Bill Lebarge, and other staff of Indian and Northern Affairs Canada, provided advice and logistical support.

Confidential proprietary data, generated by many company geologists, was supplied by Noranda, Goldnev, and Prime Explorations Ltd. We thank these companies for permission to publish their data in this paper.

Many Noranda staff and their contractors provided assistance during the study, and special thanks are due to Managers Bill Mercer (Vancouver) and Hugh Copland (Whitehorse), and the geologists who worked at Grew Creek: Heather Brown, Dennis Bull, Louise Gagnon, Ken Galambos, Jan Helsen, Sheila Reid, and Chris Wild. Alison Star produced plans, sections and data from the Grew Creek computerized database in Noranda's Vancouver office.

XRD, XRF and some ICP analyses were supplied by the laboratories at Geological Survey of Canada, Ottawa. In particular we thank Jeanne Percival, Ruth Winter, and Gina Lechaminant for XRD -, Gerry LaChance for XRF -, and Ian Jonasson for coordinating - analytical work. Colin Tinker and Andy Tulloch of DSIR Geology & Geophysics assisted with the use of the MINITAB and IGPET computer programs respectively.

Bob Brathwaite, Andy Tulloch and David Skinner reviewed the manuscript and provided constructive comments which have measurably improved the paper. The figures were drafted by Jeff Lyall and the manuscript was typed by Sue Nepe.

REFERENCES

ANON., 1985. Canyon project, Yukon Territory, 1984 - 1985 summary. Unpublished report, Hudson Bay Exploration and Development Company Limited.

BERGER, B.R., and EIMON, P., 1983. Conceptual Models of Epithermal Precious-metal Deposits. In: Cameron Volume on Unconventional Mineral Deposits, W.C. Shanks (ed.), Society of Mining Engineers of the American Institute of Mining, Metallurgical, and Petroleum Engineers, Inc., New York, p. 191-205.

BIRCH, W.D., 1978. Petrogenesis of some Palaeozoic rhyolites in Victoria. Journal of the Geological Society of Australia, Vol. 25, No. 2, p. 75-87.

BONHAM, H.F. Jr., 1986. Models for volcanic-hosted epithermal precious metal deposits; a review. Proceedings of Symposium 5: Volcanism, Hydrothermal Systems and Related Mineralization, International Volcanological Congress, February 1986, p. 13-17.

CAS, R.A.F., 1983. Submarine 'crystal tuffs': their origin using a Lower Devonian example from southeast Australia. Geological Magazine, Vol. 120, No. 5, p. 471-486.

CHRISTIE, A.B., and GORDEY, S.P., 1989. The Tintina Fault and gold: Grew Creek, Yukon. Program and Abstracts for Contributions of the Geological Survey of Canada, Cordilleran Geology and Exploration Roundup, February 7-10, 1989, Hotel Vancouver, Vancouver. Energy Mines and Resources Canada.

CHRISTIE, A.B., DUKE, J. and RUSHTON, R., 1989. Grew Creek gold deposit, Tintina Trench, Yukon. Program and Abstracts for Contributions of the Geological Survey of Canada, Cordilleran Geology and Exploration Roundup, February 7-10, 1989, Hotel Vancouver, Vancouver. Energy Mines and Resources Canada.

CLEMENS, J.D. and WALL, V.J., 1984. Origin and evolution of a peraluminous silicic ignimbrite suite: the Violet Town Volcanics. Contributions to Mineralogy and Petrology, Vol. 88, p. 354-371.

COPLAND, H., 1988a. Geochemical and geophysical report on the Canyon 37-96, 218-222, 301-347, and Grand 1-136, 138-162 claims. Unpublished report, Noranda Exploration Company Limited for the Grew Creek Development Project.

COPLAND, H., 1988b. Geochemical and geophysical report on the Canyon 7-16 and 33-36 claims. Unpublished report, Noranda Exploration Company Limited for the Grew Creek Development Project.

DIETRICH, R.V. and SKINNER, B.J., 1979. Rocks and rock minerals; John Wiley & Sons, New York, 319 p.

DUKE, J.L., 1986. The geology and alteration of the Grew Creek epithermal gold-silver occurrence in south-central Yukon Territory (105 K 2). Unpublished BSc thesis, The University of British Columbia, 65 p.

DUKE, J.L., 1988. Report on 1988 exploration activities on the Canyon and Grand claims, NTS 105 K/2, Whitehorse Mining District, latitude 62 03" N longitude 132 50" W. Unpublished report, Noranda Exploration Company Limited for the Grew Creek Development Project.

DUKE, J.L. and GODWIN, C.I., 1986. Geology and alteration of the Grew Creek epithermal gold-silver prospect, south-central Yukon. In: Yukon Geology, Vol. 1. Exploration and Geological Services Division, Yukon, Indian and Northern Affairs Canada, p. 72-82.

GORDEY, S.P. and IRWIN, S.E.B., 1987. Geology, Sheldon Lake and Tay River map areas, Yukon Territory. Geological Survey of Canada, Map 19-1987 (3 sheets), scale 1:250 000.

HAYBA, D.O., BETHKE, P.M., HEALD, P. and FOLEY, N.K., 1986. Geologic, mineralogic, and geochemical characteristics of volcanic-hosted epithermal precious-metal deposits. In: Berger, B.R., and Bethke, P.M. (eds), Geology and Geochemistry of Epithermal Systems, Society of Economic Geologists, Reviews in Economic Geology, Vol. 2, p. 129-167.

HENLEY, R.W., 1986. The geothermal framework of epithermal deposits. In: Berger, B.R., and Bethke, P.M. (eds), Geology and Geochemistry of Epithermal Systems, Society of Economic Geologists, Reviews in Economic Geology, Vol. 2, p. 1-24.

HUGHES, J.D. and LONG, D.G.F., 1980. Geology and coal resource potential of Early Tertiary strata along the Tintina Trench, Yukon Territory. Geological Survey of Canada, Paper 79-32, 21 p.

JACKSON, L.E., GORDEY, S.P., ARMSTRONG, R.L. and HARAKAL, J.E., 1986. Bimodal Paleogene volcanics near Tintina Fault, east-central Yukon, and their possible relationship to placer gold. In: Yukon Geology, Vol. 1. Exploration and Geological Services Division, Yukon, Indian and Northern Affairs Canada, p. 139-147.

LIPMAN, P.W., 1975. Evolution of the Platoro Caldera Complex and related volcanic rocks, southeastern San Juan Mountains, Colorado. United States Geological Survey Professional Paper 852.

LONG, D.G.F., 1981. Dextral strike slip faults in the Canadian Cordillera and depositional environments of related fresh-water intermontane coal basins. Geological Association of Canada Special Paper 23, p. 154-186.

MORTENSEN, J.E., 1988. Eocene magmatism in central Yukon - tectonic and metallogenic implications. Oral presentation at the Yukon Geoscience Forum, November 27-29, 1988, Whitehorse, Yukon.

PRIDE, M.J., 1988. Bimodal volcanism along the Tintina Trench, near Faro and Ross River. In: Yukon Geology, Vol. 2; Exploration and Geological Services Division, Yukon, Indian and Northern Affairs Canada, p. 69-80.

SETO, S., and CROWE, G.C., 1989. Diamond drilling report on the Grew Creek property, Grand and Canyon claims, Whitehorse Mining District, Yukon Territory. Unpublished report by Azimuth Geological Incorporated for Goldnev Resources Inc.

SKETCHLEY, D.A., 1985. Application of mineralogical and geochemical characteristics of carbonate alteration envelopes to exploration for auriferous white quartz veins at the Erickson gold mine, Cassiar, North-Central British Columbia. Proceedings of "Alteration with special reference to precious metal deposits" conference, Department of Geological Sciences, University of British Columbia, December 9, 1985, p. 1-15.

STROSHEIN, R., 1986a. The gold mineralization, geology and exploration potential at Grew Creek, Yukon Teritory. Unpublished report, Hudson Bay Exploration and Development Company Limited, January 1986.

STROSHEIN, R., 1986b. The 1986 exploration program on the Canyon project. Unpublished report, Hudson Bay Exploration and Development Company Limited, November 1986.

TABLE 1: Textural and compositional features of the three groups of rhyolitic tuffs.

NAME			COL-OUR	UNIT THICKNESS	COMPONENTS % (rounded to nearest 5%)				TEXTURE AND FABRIC					
												Average Grain Size mm		
Acro-nym	Components	Size		Avg. Maximum (section)	Crys-tal	Li-thic	Pum-ice	Ma-trix	Sorting (crystals & lithics)	Shards in matrix	Welding	Crys-tals	Lith-ics	Pum-ice
S&P	mixed crystal, lithic & vitric	coarse ash tuff, lapilli ash tuff, & lapilli tuff	Pale grey	15 54 (10300E)	40	20	10	30	moderately - well sorted	rare - absent	absent	1.5	2.5	5
CLP	mixed crystal, lithic, & vitric	coarse ash tuff & lapilli ash tuff	Med. grey	7 35 (10400 E)	20	15	15	50	moderately - poorly sorted	present	absent - moderate	1	2.5	3
VAT	vitric	ash tuff	Dark grey	1 20 (10150 E)	10	5	10	75	moderately - poorly sorted	abun-dant	absent - moderate	1	1	3

Table 2: Hydrothermal alteration types and constituent mineral assemblages

(A = abundant, M = moderate, T = trace, ± = present or absent, and Opr = overprint)

	Illite-quartz-adularia ± carbonate	Quartz-adularia	Illite-quartz	Carbonate-chlorite	Intermediate argillic	Advanced argillic
Quartz	M-A	A	A	±	M	T-M
Carbonate	T-A		±	A	relict	relict
Illite	M-A	±	Tr-M	±	relict	
Adularia	T-A	M-A	A	±	relict	
Albite	±	±	±	±		
Chlorite	±			±		
Epidote				T		
Smectite	Opr		Opr	Opr	A	±
Illite/smectite	Tr	±	±	±	±	relict
Chlorite/smectite				±		
Kaolinite	Opr		Opr	Opr	T-M	M-A
Alunite						T-M
Pyrite	T-M	T-M	T-M	T-M	T-M	T-M

TABLE 5: Diamond drill hole assay statistics

	Au	Ag	As	Hg*[2]
Number of assays	11,416	11,416	11,416	11,416
Mean (average) ppm	0.35	1.45	62.2	0.32
50th percentile (median) ppm	<0.07*[1]	<0.7*[1]	25	0.09
90th percentile ppm	0.35	1.4	115	0.68
96th percentile ppm	1.0	3.4	235	1.5
Maximum value ppm	183.5	907.2	1262.0	12.8*[2]
Standard deviation ppm	-	-	88.70	0.75
Detection limit ppm	0.07	0.7	2	0.01

Analyses from DDH1-DDH90 but excluding DDH17 and DDH65. Statistical analysis calculated using MINITAB on Digital Equipment Corp. VAX mainframe computer

*[1] Below detection limits. Extrapolation of cumulative frequency curves (Fig. 18) suggest means of approximately 0.03 ppm for Au and 0.25 ppm for Ag.

*[2] Most analyses of >5 ppm Hg samples were recorded as 5 ppm and therefore samples more concentrated than the 12.8 ppm maximum value may be present.

TABLE 6: Regression analyses of drillhole assay data

Element pair	Number of Assays	Regression equation	R-sq*
Au-Ag	2,771	Au= 0.521 + 0.158 Ag	50.6%
Ag-Hg	2,771	Ag= - 1.00 + 13.5 Hg	18.0%
Au-Hg	2,771	Au= 0.125 + 2.68 Hg	14.6%
As-Hg	11,416	As= 56.6 + 18.4 Hg	2.4%
Au-As	2,771	Au= 1.53 - 0.00185 As	0.1%
Ag-As	2,771	Ag= 5.62 - 0.00633 As	0.1%

Regression analyses carried out using MINITAB on Digital Equipment Corp. VAX mainframe computer

* R-sq is a measure of how well the regression equation fits the data, with 100% indicating a perfect fit.

$$\text{R-sq} = \text{R- squared} = \frac{100 \text{ (sum of squares due to regression)}}{\text{(sum of squares total)}}$$

Table 3: Average whole rock analyses of Eocene basalts and rhyolites (calculated free of water and carbon dioxide but LOI noted to give indication of alteration).

	B A S A L T S									R H Y O L I T E S				
Location	Grew Ck.	Grew Ck.	Grew Ck.	Glenlyon	Ketza R.	Weasel Ck.	Hoole R.	Pillow Mt	L.Starr Ck.	Grew Ck.	Glenlyon[1]*	Glenlyon[2]*	Riddle R.	Tay R.
Source**	1	2	3	3	3	4	4	4	4	1	3	3	4	4
Number of analyses	9	2	3	19	3	1	1	1	1	6	8	5	1	1
LOI***	12.45	3.45	1.44	5.45	1.98	1.38	3.18	3.21	2.82	3.38	1.34	1.85	0.7	1.6
S_iO_2	48.36	49.32	50.30	49.77	50.89	49.77	51.79	50.65	51.83	77.93	75.01	72.06	75.33	76.32
TiO_2	2.43	2.42	2.34	2.15	2.62	1.84	2.41	2.25	2.14	0.25	0.03	0.29	0.07	0.13
Al_2O_3	17.61	16.70	15.95	16.50	14.65	15.63	16.04	15.07	16.50	12.65	11.93	12.90	13.40	12.09
Cr_2O_3	0.02													
Fe_2O_3T	11.74		11.72	11.38	12.40					2.26	0.16	2.81		
Fe_2O_3	1.75	4.01				2.18	4.38	3.66	4.42	0.19			1.00	1.00
FeO	9.01	6.57				8.52	5.67	7.50	5.72	1.88			1.00	0.90
MnO	0.18	0.51	0.21	0.18	0.19	0.16	0.17	0.21	0.14	0.05	1.34	0.07	0.02	0.02
MgO	5.13	4.64	5.26	5.18	4.91	8.06	4.50	5.26	4.51	0.33	0.41	0.17	0.04	0.12
CaO	8.18	7.98	8.02	9.03	8.62	8.74	8.96	8.67	9.02	0.94	3.12	0.66	0.90	0.36
Na_2O	4.15	3.74	3.67	2.83	2.88	2.72	3.14	2.51	3.00	0.45	5.21	2.88	3.79	2.03
K_2O	2.32	1.69	1.53	1.33	1.43	1.02	1.43	1.57	1.29	4.95	0.18	5.80	5.45	5.08
P_2O_5	0.66	0.60	0.42	0.70	0.85	0.44	0.84	0.71	0.58	0.03	0.04	0.04	0.02	0.04
Ba	708		923	810	788	401	733	553	581	333	620	660	10	41
Nb	58		47	34	44					52	84	58		

Rb	79		68	45	51					295	356	290		
Sr	647		599	580	374	283	385	329	326	58	50	39		
Y	51									123				
Zr	270		241	260	384					400	550	598		
Be	4.5					0.5	1.0	0.5	0.5	4.2			8.7	6.6
Co	42		36	34	22	29	23	23	22	25	1	2	3	3
Cr	144		148	154	166	210	164	156	122	8	30	28	6	6
Cu	46		29	20	19	38	49	37	43	8	3	2	18	11
La	38									90			57	63
Ni	72		61	53	24	67	41	38	42	9	2	2	7	9
Pb	1					1	1	1	1	42			63	30
V	190					140	140	146	159	7			11	3
Yb	2.54									9.4			11.0	2.8
Zn	90					86	86	97	86	81			121	84
Ag						0.6	0.2	0.2	0.2				1.0	1.0

* Glenlyon 1 = low K rhyolites, Glenlyon 2 = high K rhyolites

** Source: 1 = this study, 2 = Duke and Godwin (1986), 3 = Pride (1988), and 4 = Jackson et al. (1986)

*** LOI = loss on ignition (H_2O + CO_2 + S)

Table 4: Multi-element assays for DDH 29 and DDH 30

DDH29*

DEPTH m	Au ppm (FA)*3	Ag ppm (FA)*3	Ag ppm (ICP)*4	Cu ppm	Pb ppm	Zn ppm	Mo ppm	Ni ppm	Co ppm	Mn ppm	Fe %	As ppm	Sb ppm	Bi ppm	W ppm
36.6-42.6	0.81	1.03	1.2	8	13	65	1	9	4	151	2.48	101	7	2	2
42.6-48.6	0.22	0.53	0.3	8	18	72	1	8	4	375	2.23	45	3	2	1
48.6-54.6	0.06	0.35	0.1	9	26	100	2	7	6	427	2.96	56	2	2	1
54.6-60.6	0.19	0.35	0.1	8	28	101	2	6	5	518	2.93	54	2	2	1
60.6-66.6	0.1	0.35	0.2	8	23	86	2	7	4	439	2.23	47	2	2	1
66.6-72.6	15.43	159.4	163.1	10	21	71	4	6	4	553	2.21	164	5	2	1
72.6-78.6	30.48	218	274.4	20	18	71	3	5	2	412	1.25	55	2	2	16
78.6-84.6	34.72	175.4	191.8	13	21	63	2	5	3	378	1.44	114	4	2	1
84.6-90.6	36.78	237.5	272.4	11	25	70	4	5	3	340	1.35	100	3	2	1
90.6-96.6	1.96	3.6	2.3	8	21	74	1	4	3	382	1.61	110	2	2	1
96.6-102.6	2.12	3.4	2.7	13	22	74	2	7	4	411	1.86	171	2	2	4
102.6-108.6	0.95	2.1	1.9	8	17	71	1	9	5	510	2.23	133	2	2	1
108.6-114.6	0.59	1.5	1.6	8	20	62	2	5	4	388	1.53	110	2	2	1
114.6-120.6	0.7	2.1	2.2	8	15	50	1	6	3	301	1.25	73	2	2	1
120.6-126.6	0.37	1.2	1.4	11	16	62	1	8	4	309	1.47	105	3	2	1
126.6-132.6	0.33	3.1	0.9	8	20	70	2	4	2	275	1.31	115	2	3	1
132.6-138.6	0.28	0.78	0.8	10	14	66	2	16	8	488	2.25	138	4	3	1
138.6-142.6	0.46	1.1	1	8	16	61	1	8	4	448	1.94	154	3	2	1

Table 4 (contd)

DDH30[*2]

DEPTH m	Au ppm (FA)[*3]	Ag ppm (FA)[*3]	Ag ppm (ICP)[*4]	Cu ppm	Pb ppm	Zn ppm	Mo ppm	Ni ppm	Co ppm	Mn ppm	Fe %	As ppm	Sb ppm	Bi ppm	W ppm
53.6-59.6	0.03	0.35	0.1	50	16	97	2	60	15	731	4.21	65	24	4	1
59.6-65.6	0.04	0.35	0.2	27	19	85	1	50	11	326	2.81	70	18	2	1
65.6-71.6	0.56	0.61	0.5	58	52	67	1	27	8	132	2.45	170	27	2	1
71.6-77.6	0.04	0.35	0.1	12	43	205	1	10	6	267	3.47	27	7	2	1
77.6-83.6	0.45	0.43	0.1	8	25	78	1	5	3	602	1.27	75	2	2	1
83.6-89.6	0.21	0.35	0.1	7	26	85	1	6	4	567	2.11	103	2	2	1
89.6-95.6	0.03	0.35	0.1	8	34	107	3	8	5	242	2.73	17	2	2	1
95.6-101.6	0.07	0.35	0.1	8	33	99	8	8	5	228	2.37	69	2	2	1
101.6-107.6	0.14	0.63	0.4	6	27	80	9	6	4	581	1.92	71	2	2	1
107.6-113.6	0.47	2.93	2.7	8	28	82	5	6	4	576	1.94	88	2	2	1
113.6-119.6	7.3	34.63	35.7	6	28	67	4	5	4	558	1.72	84	2	3	1
119.6-125.6	1.2	2.58	2.7	47	25	70	3	7	3	288	1.17	108	3	2	1
125.6-131.6	22.04	22.78	29.6	8	18	40	1	6	4	670	2.06	64	2	2	1
131.6-137.6	0.57	1.98	1.1	5	20	71	2	8	4	393	1.52	45	2	2	1
137.6-143.6	0.09	0.7	0.6	9	21	70	2	7	5	408	1.78	62	2	2	1
143.6-149.6	0.16	0.7	0.4	6	20	62	1	8	5	423	1.85	75	2	2	1
149.6-155.6	0.15	0.7	0.6	7	18	62	1	7	4	439	1.96	70	2	2	1
155.6-161.6	0.16	0.7	0.5	8	22	66	1	9	5	508	2.27	73	2	2	1
161.6-167.6	0.25	0.88	0.7	6	24	62	1	7	5	470	2.03	70	2	2	1
167.6-173.6	0.11	1.13	0.9	9	24	72	1	9	6	554	2.26	99	2	2	1
173.6-179.6	0.13	0.68	0.6	9	23	70	1	9	6	409	2.04	147	2	2	1
179.6-185.6	0.04	0.35	0.1	16	21	77	2	22	9	673	3.18	113	2	2	1
185.6-188.9	0.03	0.35	0.1	9	22	76	2	9	7	576	2.54	48	2	2	1

*DDN29: Section 10175E (Fig. 3), length 142.65m, bearing 199° and dip 45°.

*2DDN30: Section 10175E (Fig. 3), length 188.98 m, bearing 199° and dip 45°.

*3FA = fire assay

*4ICP = ICP analyses by Acme Analytical Laboratories Ltd, Vancouver. 0.5 grams of sample were digested with 3 ml 3-1-2 HCl-HN03-$H_2$0 at 95°C for one hour and diluted with 10 ml of $H_2$0.

APPENDIX: XRF and XRD analyses of Grew Creek samples

Rock Type		Basalt									Diabase (diorite)		
Sample No.	DL	39-149.8	55-30.7	57-58.8	66-96.1	66-115.2	72-117.2	71-135.3	83-58.7	83-62.5	67-355.8	90-44.7	90-58.85
Density (kg/m³)		2700	2830	2680	2770	2740	2740	2740	2740	2770	2610	2760	2740
Lab. No.		63	1,67,68	2,72,73,74	3,82,83	84	84	4,90,91	5,94,95	6,96	86	43	44
No. of analyses		1	3	4	3	1	1	3	3	2	1	1	1
WHOLE ROCK XRF ANALYSES													
SiO2 %	0.40**	46.60	46.13	44.88	42.30	32.60	44.80	42.60	41.43	39.75	47.20	45.30	46.20
TiO2 %	0.02	2.31	2.08	2.21	2.10	1.77	1.87	2.11	2.30	2.40	1.94	2.01	2.05
Al2O3 %	0.40	20.10	15.40	15.50	15.27	12.60	14.20	15.07	15.60	15.00	15.00	12.70	15.30
Cr2O3 %	0.02	0.04	0.01	0.01	0.01	0.01	0.01	0.02	0.02	0.02	0.06	0.01	0.01
Fe2O3T %	0.10	6.40	10.33	10.88	10.80	9.90	9.70	10.47	11.37	12.65	9.70	9.90	10.20
Fe2O3 %		0.50	1.80	2.63	1.70	0.80	0.70	2.47	1.50	1.65	1.10	0.80	3.50
FeO %	0.20	5.30	7.77	7.43	8.20	8.20	8.10	7.20	8.90	9.90	7.70	8.20	6.00
MnO %	0.01	0.11	0.17	0.18	0.17	0.15	0.16	0.15	0.21	0.12	0.13	0.14	0.15
MgO %	0.10	1.45	4.19	3.77	3.51	8.20	4.77	5.21	4.23	5.12	4.39	4.66	2.05
CaO %	0.10	3.62	6.92	7.27	8.70	9.22	4.61	7.99	8.55	7.58	5.61	6.17	6.86
Na2O %	0.50	3.50	4.03	3.88	3.53	3.20	4.00	3.50	3.53	3.50	4.20	1.70	2.10
K2O %	0.05	5.56	2.16	1.91	1.72	1.32	1.78	1.92	0.94	0.99	0.83	2.48	2.66
H2OT %	0.10	2.50	0.43	2.05	1.30	1.80	1.90	2.37	1.93	2.35	1.70	2.00	2.80
CO2T %	0.05	6.50	8.30	7.98	10.53	20.10	12.10	9.00	10.43	10.50	10.00	13.80	9.80
P2O5 %	0.02	0.43	0.52	0.56	0.71	0.63	0.49	0.57	0.64	0.68	0.46	0.60	0.59
S %	0.04	0.49	0.03	0.06	0.05	0.04	0.08	0.07	0.08	0.20	0.03	0.04	0.00
Ba ppm		268	824	819	954	500	139	631	727	725	334	232	510
Nb ppm		40	55	59	52	42	49	56	48	59	49	67	66
Rb ppm		208	40	54	71	54	54	43	41	57	81	114	157
Sr ppm		201	608	645	829	320	289	757	748	680	335	214	230
Y ppm		56	32	41	46	30	32	43	74	49	46	56	57
Zr ppm		265	265	284	227	121	229	267	226	240	253	329	330
TOTAL		99.00	100.12	100.51	100.02	100.80	99.70	100.43	100.48	99.94	100.40	100.80	100.20
WHOLE ROCK ICP ANALYSES													
Be ppm	0.50	14.0	2.0	2.3	2.6	2.5	5.9	2.3	1.8	1.7	1.3	6.3	3.4
Co ppm	5	61	35	34	35	28	28	36	40	35	44	29	32
Cr ppm	10	300	92	101	91	71	100	115	140	125	340	88	84
Cu ppm	10	68	30	33	38	28	45	48	37	37	41	32	36
La ppm	10	21	39	40	35	28	30	35	32	38	20	30	34
Ni ppm	10	88	43	52	59	51	73	82	67	54	75	55	52
Pb ppm	20	3				3	0				2	7	14
Sr ppm		200	610	650	850	320	290	765	755	680	340	210	230
V ppm	5	240	167	170	153	110	140	173	173	170	160	120	150
Yb ppm	0.50	4.20	2.40	2.30	2.00	1.50	1.50	2.00	1.90	2.20	2.60	3.00	3.20
Zn ppm	5	110	87	95	69	61	56	76	72	85	68	79	82
WHOLE ROCK XRD ANALYSES													
		PLAG	K-FELD	PLAG	PLAG	PLAG	PLAG	plag	PLAG	PLAG	PLAG	qtz	qtz
		K-FELD	PLAG	K-FELD	K-FELD	K-FELD	qtz	K-feld	sid	sid	K-FELD	plag	plag
		ca	sid	(qtz)	sid	DOL	sid	sid	dol	(qtz)	qtz	sid	ca
		sid	(qtz?)	(ca)	(qtz)	sid	dol	(qtz)	(qtz?)	(ca)	sid	dol	sid
		(mica)	(py?)	(sid)	(ca)	(qtz)	(ca)	(ca)	(ca?)	chl/clay	dol	chl/clay	(mica)
							chl/clay?	(dol?)	chl/clay				
CLAY SEPARATE XRD ANALYSES													
		ILL	SID	CHL	SM	ILL	ILL	CHL	CHL	CHL	ILL	ILL	ILL
		(ill/sm)	PLAG	PLAG	ch	PLAG	PLAG	chl/sm	plag	plag	CHL	KFELD	plag
			qtz	sid	sid	K-FELD	chl	ill	sid	ill	K-feld		ca
			(dol?)	qtz	plag	(ill/sm)	(qtz)	ca	(qtz)	sid	sid		kaol
				ca	(ca)	anatase?	(py)	qtz	(py)	ca	qtz		qtz
				chl/sm	(qtz)		(ill/sm)	sid	(ill/sm)	(qtz)			(py)
					(py)				(dol?)	(ill/sm)			

Rock Type	Basaltic tuffs					Rhyolite					
Sample No.	63-66.2	82-307	55-188.3	61-99.15	63-67.1	17-347.1	50-104.3	90-83.3	90-98.6	90-142.1	90-218.3
Density (kg/m³)	2.65	2600	2570	2550	2630	2570	2530		2390	2520	2550
Lab No.	77	93	70	76	78	53	66	45	46	47	48
No. of Analyses	1	1	1	1	1	1	1	1	1	1	1

WHOLE ROCK XRF ANALYSES

SiO_2 %	42.90	51.00	55.70	41.40	52.90	70.70	76.20	75.30	79.20	76.20	74.20
TiO_2 %	1.77	2.00	1.03	1.76	1.48	0.40	0.36	0.23	0.08	0.13	0.25
Al_2O_3 %	13.80	16.20	10.70	13.60	13.90	10.80	12.50	10.80	11.10	14.50	13.60
Cr_2O_3 %	0.01	0.02	0.01	0.02	0.01	0.00	0.00	0.00	0.00	0.00	0.00
Fe_2O_3T %	9.50	9.20	6.50	10.00	8.30	4.50	1.00	2.30	1.40	1.70	2.20
Fe_2O_3 %	1.00	0.70	0.20	0.80	0.90	0.00	0.00	0.00	0.00	0.70	0.40
FeO %	7.70	7.60	5.70	8.20	6.70	4.00	0.90	2.10	1.30	0.90	1.70
MnO %	0.15	0.13	0.11	0.17	0.11	0.11	0.00	0.03	0.03	0.02	0.09
MgO %	4.92	2.74	3.52	5.47	3.64	0.64	0.43	0.33	0.17	0.18	0.16
CaO %	6.67	3.59	5.59	6.71	3.57	1.18	0.44	2.24	0.16	0.59	0.85
Na_2O %	3.90	3.10	0.60	3.10	2.80	0.30	0.40	0.20	1.40	0.10	0.20
K_2O %	1.64	2.17	4.51	2.18	2.48	5.07	5.39	3.12	4.86	4.40	5.85
H_2OT %	2.20	3.60	1.30	2.20	2.30	1.40	2.20	1.60	0.90	2.00	1.40
CO_2T %	12.80	6.90	10.90	14.40	9.00	3.90	0.70	3.00	0.90	0.60	1.70
P_2O_5 %	0.58	0.53	0.26	0.47	0.36	0.06	0.05	0.03	0.01	0.02	0.03
S %	0.36	0.14	0.13	0.20	0.18	0.09	0.02	0.02	0.03	0.18	0.03
Ba ppm	320	574	449	330	543	587	687	122	171	24	340
Nb ppm	46	49	30	46	44	40	44	48	38	78	54
Rb ppm	54	62	188	73	89	184	259	184	288	457	340
Sr ppm	357	350	187	274	266	120	111	66	0	0	37
Y ppm	38	40	38	68	47	88	111	108	82	218	108
Zr ppm	234	268	228	195	265	567	416	428	146	295	466
TOTAL	**100.50**	**100.60**	**100.40**	**100.80**	**100.40**	**99.70**	**99.70**	**99.10**	**100.20**	**100.70**	**100.50**

WHOLE ROCK ICP ANALYSES

Be ppm	6.3	4.1	10.0	7.9	6.5	3.0	5.8	3.8	2.1	6.1	3.9
Co ppm	33	33	25	36	30	24	13	29	33	16	28
Cr ppm	87	120	69	110	76	13	16	8	6	7	8
Cu ppm	41	43	25	43	31	6	12	7	6	10	6
La ppm	39	37	38	35	45	91	92	110	35	92	100
Ni ppm	73	70	45	78	59	14	12	9	5	6	7
Pb ppm	11	15	13	5	12	29	22	37	50	65	43
Sr ppm	360	350	190	270	270	120	110	66	0	0	37
V ppm	130	170	96	150	130	12	18	5	1	2	3
Yb ppm	2.00	2.50	2.80	1.90	2.70	6.40	7.70	8.30	7.20	17.00	8.10
Zn ppm	69	68	58	81	68	88	54	100	52	92	85

WHOLE ROCK XRD ANALYSES

	PLAG	plag	qtz	dol	NA-FELD	qtz	QTZ	QTZ	QTZ	QTZ	QTZ
	sid	qtz	sid	plag	qtz	K-feld	K-feld	mica	K-feld	K-MICA	mica
	dol	(ca)	dol	sid	sid	(mica)	(mica)	sid	plag		K-feld
	(qtz)	(sid)	(feld)	(qtz)	(mica)	(ca)		(ca)	(sid)		
	(mica)	chl/clay?	(mica)	(mica)	(ca)				(mica?)		
	(ca)		(ca)		chl/clay?						
	chl/clay?				(dol?)						

CLAY SEPARATE XRD ANALYSES

	PLAG	CHL	ILL	ILL	ILL	ILL	ILL	ILL	ILL	ILL	ILL
	ILL	ILL	K-FELD	PLAG	K-FELD	K-FELD	K-FELD	(qtz)	plag	QTZ	K-FELD
	CHL	PLAG	sid	chl	PLAG	qtz	qtz	(ca)	qtz	plag	qtz
	K-feld	K-feld	qtz	(sid)	chl	sid	(ill/sm)	(sid)	(ill/sm?)		ca
	sid	qtz	(ill/sm)	(qtz)	sid	(ill/sm)		(ill/sm?)			(ill/sm)
	dol	sid		(dol)	qtz						(sm)
	ca	(ca)		(ill/sm)	(ill/sm)						
	qtz	(ill/sm)		(py)							
	(ill/sm)										
	(hem or py)										

Rock Type	VA tuff						CLP tuff					
Sample No.	18-	23-106.8	72-172.8	85-33.4	29-84.3	65-123.3	17-113.7	18-159.6	28-97.7	35-36.5	38-143.6	40-193.8
Density (kg/m³)	311.9	2380	2510	2540		2510	2540	2380	2400			
Lab. No.		57	92	42	59	81	49	54	58	60	61	64
No. of analyses	52	1	1	1	1	1	1	1	1	1	1	1
	1											

WHOLE ROCK XRF ANALYSES

SiO_2 %	76.30	72.80	75.90	71.70	80.50	74.70	72.60	76.30	80.80	79.80	80.50	74.40
TiO_2 %	0.38	0.32	0.28	0.31	0.27	0.33	0.42	0.40	0.41	0.38	0.22	0.26
Al_2O_3 %	9.90	10.00	10.10	12.50	10.10	12.80	11.90	10.80	9.20	9.00	7.30	8.20
Cr_2O_3 %	0.00	0.00	0.00	0.00	0.00	0.00	0.00	0.00	0.00	0.00	0.00	0.00
Fe$_2$O$_3$T %	4.00	3.60	2.30	3.10	0.90	1.50	3.70	2.80	1.50	2.00	3.10	3.10
Fe_2O_3 %	0.50		0.00	0.10	0.00	0.00		0.20	0.20	0.20	0.00	
FeO %	3.10		2.20	2.70	1.00	1.50		2.30	1.20	1.60	2.90	
MnO %	0.05	0.06	0.05	0.04	0.02	0.02	0.02	0.05	0.02	0.03	0.07	0.08
MgO %	0.74	0.67	0.75	0.65	0.29	0.52	0.64	0.40	0.43	0.36	0.52	0.95
CaO %	0.62	0.27	1.02	1.18	0.13	0.26	0.62	0.31	0.30	0.21	0.21	2.81
Na_2O %	0.40	0.20	0.80	1.40	0.20	0.80	0.60	0.40	0.50	0.20	0.20	0.20
K_2O %	3.11	5.42	3.66	5.05	5.53	3.84	4.98	5.30	4.61	6.14	3.52	5.20
H$_2$OT %	1.70		1.70	1.40	1.10	2.50		1.40	1.20	0.80	1.10	
CO_2T %	2.80	1.70	3.60	3.00	0.70	2.60	0.80	1.80	0.80	1.30	2.30	4.10
P_2O_5 %	0.10	0.10	0.07	0.08	0.07	0.08	0.12	0.11	0.15	0.10	0.07	0.07
S %	0.41	1.01	0.01	0.29	0.25	0.01	2.78	0.40	0.47	0.32	0.24	1.16
Ba ppm	267	410	345	653	399	355	633	589	496	426	296	325
Nb ppm	26	30	32	40	37	41	32	25	24	24	29	24
Rb ppm	156	261	163	211	290	183	207	212	190	328	177	248
Sr ppm	57	76	31	67	44	84	64	88	60	46	35	90
Y ppm	66	69	83	93	83	116	71	71	53	52	71	50
Zr ppm	264	341	326	421	364	398	420	368	293	338	259	279
TOTAL	**100.10**	**96.20**	**100.10**	**100.60**	100.30	100.10	99.20	100.30	**100.40**	**100.50**	99.30	100.60

WHOLE ROCK ICP ANALYSES

Be ppm	3.5	6.8	5.2	4.6	7.8	7.6	6.0	5.7	7.3	6.7	8.0	5.5
Co ppm	20	25	17	17	32	13	24	25	36	31	32	16
Cr ppm	32	21	17	15	13	17	22	23	24	21	18	17
Cu ppm	7	8	13	9	6	10	9	8	8	6	8	6
La ppm	46	65	74	91	75	97	69	60	49	50	64	45
Ni ppm	16	13	16	13	9	10	14	13	15	11	13	13
Pb ppm	27	28	20	46	27	30	31	24	16	20	25	21
Sr ppm	57	76	31	67	44	84	64	88	60	46	35	90
V ppm	36	27	26	20	14	21	28	30	26	27	22	18
Yb ppm	4.30	5.10	6.40	6.60	5.90	8.20	5.40	4.90	3.70	4.00	5.30	3.80
Zn ppm	61	60	74	54	74	88	70	63	56	57	59	63

WHOLE ROCK XRD ANALYSES

	QTZ	QTZ	QTZ	QTZ	QTZ	QTZ	QTZ	QTZ	QTZ	QTZ	QTZ	QTZ
	K-feld	K-FELD	(mica)	K-FELD	K-FELD	mica	K-fekl	K-FELD	K-FELD	K-FELD	K-FELD	K-feld
	sid	(sid?)	(plag)	PLAG		(plag)	(mica)	(mica)	(mica?)			dol/ank
	(mica)			(mica)		(K-feld)						(ca)
	(ca)			(sid?)		(sid)						

CLAY SEPARATE XRD ANALYSES

	ILL	ILL	ILL	ILL	K-FELD	ILL	K-FELD	ILL	ILL	K-FELD	K-FELD	K-FELD
	KFELD	K-FELD	K-FELD	PLAG	ILL	QTZ	ILL	K-FELD	K-FELD	ILL	ILL	ILL
	qtz	qtz	qtz	qtz	qtz	K-FELD	qtz	qtz	qtz	qtz	qtz	qtz
	sid	(ill/sm)	plag	sm	(ill/sm)	ill/sm	sid	sid	(ill/sm)	(ill/sm2)	sid	(ill/sm)
	(ill/sm)		(sid)	(ill/sm)			ca	(ill/sm)		(sid?)	(ill/sm)	(dol?)
			(ill/sm)				(ill/sm)					

Appendix (continued): XRD and XRF analyses of Grew Creek samples

Rock Type	CLP tuff (continued)				S & P tuff					Hydro-thermal	-breccia	Quartz vein
Sample No.	64-57.9	64-68.2	66-165.4	68-262.4	17-221.5	17-291.9	39-90	56-264.4	60-200.4	55-183.8	21-61.7	29-74.90
Density (kg/m³)	2.44	2500	2500	2500	2510	2470		2480	2600	2490		
Lab. No.	79	80	85	87	50	51	62	71	75	69	56	(27)
No. of analyses	1	1	1	1	1	1	1	1	1	1	1	1

WHOLE ROCK XRF ANALYSES

SiO_2 %	74.60	66.10	74.50	71.80	74.80	68.90	74.60	64.00	65.10	70.10	76.30	79.60
TiO_2 %	0.40	0.52	0.41	0.44	0.52	0.55	0.48	0.70	0.60	0.35	0.30	0.01
Al_2O_3 %	12.70	16.40	12.10	13.00	11.00	12.80	10.80	12.80	13.00	8.60	8.00	7.30
Cr_2O_3 %	0.00	0.00	0.00	0.00	0.00	0.00	0.00	0.00	0.00	0.00	0.00	0.00
Fe_2O_3T %	1.70	3.90	3.30	1.40	2.00	4.00	2.10	5.20	4.80	7.00	4.20	1.10
Fe_2O_3 %	0.20	0.60	0.30		0.10	0.10		0.40	0.40	0.20		
FeO %	1.30	3.00	2.70		1.70	3.50		4.40	4.00	6.10		
MnO %	0.03	0.07	0.06	0.06	0.03	0.06	0.01	0.11	0.09	0.18	0.11	0.07
MgO %	0.58	1.04	0.04	0.70	0.44	1.01	0.49	1.10	0.82	1.22	0.85	1.11
CaO %	0.81	0.86	0.66	1.19	1.34	1.31	0.52	2.98	2.69	1.53	0.84	2.32
Na_2O %	0.70	0.90	0.70	0.60	1.30	1.30	0.40	1.50	1.80	0.20	0.10	0.10
K_2O %	4.18	5.55	4.77	5.68	5.34	4.86	5.20	4.71	5.23	4.31	5.25	5.67
H_2OT %	2.30	2.30	1.70	1.80	0.90	1.60		1.40	1.20	1.10		0.30
CO_2T %	1.50	2.80	2.20	2.00	2.10	3.80	0.70	5.70	5.10	5.60	2.30	3.40
P_2O_5 %	0.10	0.12	0.09	0.11	0.14	0.13	0.12	0.17	0.14	0.11	0.07	0.00
S %	0.25	0.13	0.19	0.66	0.39	0.04	1.22	0.07	0.02	0.48	1.78	0.02
Ba ppm	485	646	704	811	678	802	576	530	761	420	375	124
Nb ppm	35	51	34	35	24	27	27	33	29	24	24	0
Rb ppm	186	275	191	253	205	176	219	192	187	204	286	326
Sr ppm	148	220	131	83	50	96	102	88	113	71	69	58
Y ppm	83	115	80	93	50	58	56	72	64	59	51	14
Zr ppm	392	469	376	455	355	399	387	407	397	295	267	38
TOTAL	**99.70**	**100.60**	**100.90**	**99.60**	**110.20**	**100.10**	**96.70**	**100.20**	**100.40**	**100.30**	**100.30**	**101.00**

WHOLE ROCK ICP ANALYSES

Be ppm	5.3	8.1	5.0	7.0	4.4	2.9	5.7	3.4	3.9	65.0	15.0	24
Co ppm	15	16	17	22	32	26	76	31	25	20	44	2
Cr ppm	21	26	23	22	25	34	31	43	40	31	24	11
Cu ppm	11	9	10	7	11	8	10	11	10	9	9	16
La ppm	81	110	73	78	49	55	58	55	59	47	52	0
Ni ppm	14	19	17	14	19	21	18	24	28	17	16	6
Pb ppm	21	34	14	21	26	23	25	26	21	21	24	
Sr ppm	150	220	130	83	50	96	100	88	110	71	69	
V ppm	21	35	34	25	29	38	24	53	45	47	22	3
Yb ppm	6.30	8.60	5.70	6.10	3.50	3.90	4.00	4.60	4.40	4.10	3.60	0.90
Zn ppm	33	140	73	82	53	68	67	84	73	78	60	11

WHOLE ROCK XRD ANALYSES

	QTZ	qtz	QTZ	QTZ	QTZ	QTZ	QTZ	qtz	K-FELD	QTZ	QTZ	
	(mica)	mica	mica	K-feld	K-FELD	K-FELD	K-FELD	K-feld	ca	K-feld	K-FELD	
	(plag)	plag	plag	(mica)	PLAG	PLAG	(mica?)	plag	qtz	sid	(py)	
	(K-feld)	K-feld	(sid)	(dol)	(mica)	sid		ca	sid	(mica?)		
	(dol)	(sid)		(py)		(mica)		sid				
						(ca)		(mica)				

CLAY SEPARATE XRD ANALYSES

	ILL	ILL	ILL	ILL	K-FELD	ILL	ILL	ILL	ILL	ILL	ILL	
	K-FELD	qtz	K-FELD	K-FELD	ILL	K-FELD	K-FELD	sid	plag	K-FELD	K-FELD	
	qtz	(ill/sm)	QTZ	qtz	qtz	qtz	qtz	ca	qtz	sid	qtz	
	(ill/sm)		sid	(ill/sm)	plag	(ill/sm)	(ill/sm)	qtz	sm	qtz	(ill/sm)	
			(ill/sm2)		(m-lay)			(ill/sm)	ca	(ill/sm)		
									(ill/sm)			

All analyses by Geological Survey of Canada laboratories, Ottawa. XRF analyses on fused disks except FeO, H_2OT, CO_2T, and S by wet chemical techniques.

Fe_2O_3 is calculated using: $Fe_2O_3 = Fe_2O_3T$ (XRF) - 1.11134 X FeO (volumetric) ICP analyses are Geological Survey of Canada's ICP-TR1 group obtained on 1.0 gram of sample (acid + fusion of residue) dissolved in 10% HCl and diluted to 100 ml. Interpretation of XRD diffractograms was by J.B. Percival of Geological Survey of Canada. For clay separates, analyses were made of untreated, heated and glycolated samples to aid interpretation of the clay minerals present.

XRD quantitative estimates: ILL = abundant, ill = minor, (ill) = trace, and (ill?) = trace, tentative identification

XRD abbreviations: ank = ankerite, ca = calcite, chl = chlorite, dol = dolomite, feld = feldspar, ill = illite, kaol = kaolinite, plag = plagioclase, py = pyrite, qtz = quartz, sid = siderite, and sm = smectite

* Column of analytical detection limits